ISBN: 978-93-47587-12-2

GREEN SYNTHESIS OF NANO FERRITES FROM DIFFERENT PLANT LEAVES

CHARACTERIZATION AND APPLICATIONS AS PHOTO DEGRADATION ACTIVITY

MR. RAHUL KUMAR
DR. BASSA SATYANNARAYANA

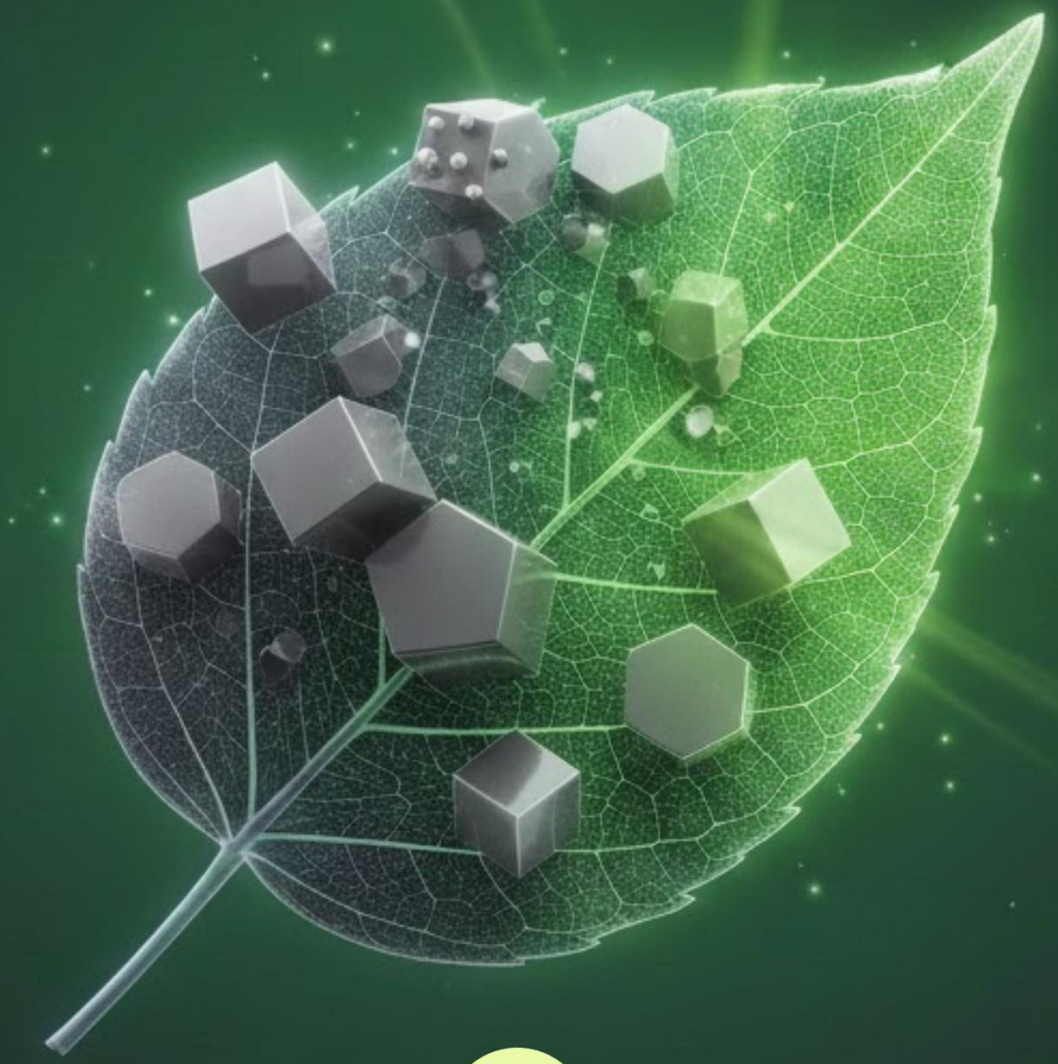

Bhumi Publishing, India
First Edition: January 2026

GREEN SYNTHESIS OF NANO FERRITES FROM DIFFERENT PLANT LEAVES, CHARACTERIZATION AND APPLICATIONS AS PHOTO DEGRADATION ACTIVITY

(ISBN: 978-93-47587-12-2)

DOI: https://doi.org/10.5281/zenodo.18193648

Authors

Mr. Rahul Kumar

Department of Environmental Studies,

Indira Gandhi National Open University, Bhopal

Dr. Bassa Satyannarayana

Assistant Professor & HOD,

Department of Chemistry, Govt. M.G.M P.G. College, Itarsi

E-mail: satya.bassa@gmail.com

Bhumi Publishing

Januray 2026

Title: Green Synthesis of Nano Ferrites from Different Plant Leaves,
Characterization and Applications as Photo Degradation Activity

Authors: Mr. Rahul Kumar and Dr. Bassa Satyannarayana

First Edition: January 2026

ISBN: 978-93-47587-12-2

DOI: https://doi.org/10.5281/zenodo.18193648

Published by Bhumi Publishing,

a publishing unit of Bhumi Gramin Vikas Sanstha

Bhumi Publishing

Nigave Khalasa, Tal – Karveer, Dist – Kolhapur, Maharashtra, INDIA 416 207

E-mail: bhumipublishing@gmail.com

Disclaimer: The views expressed in the book are of the authors and not necessarily of the publisher and editors. Authors themselves are responsible for any kind of plagiarism found in their chapters and any related issues found with the book.

PREFACE

"Green Synthesis of Nano Ferrites from Different Plant Leaves, Characterization and Applications as Photo Degradation Activity" provides an overview of the work's purpose, environmental significance, and range of results.

A brief draft designed for this kind of research is provided below, highlighting the transition to sustainable nanotechnology in 2025.

Environmental clean-up has been transformed by the quick development of nanotechnology, yet the conventional physical and chemical processes for creating nanoparticles frequently use hazardous chemicals and a lot of energy. An environmentally safe substitute is investigated in this work: the green synthesis of Nano ferrites utilizing extracts from different plant leaves.

This study shows a sustainable and economical technique to create high-performance magnetic nanoparticles by exploiting the natural reducing and stabilizing qualities of phytochemicals, such as phenols, flavonoids, and terpenoids.

The study is designed to offer:

- Eco-Friendly Synthesis: Comprehensive procedures for making nano ferrites from a variety of plant sources, removing dangerous solvents and surfactants.
- Comprehensive Characterization: Verifying the spinel structure, shape, and purity of the produced nanoparticles using cutting-edge methods like XRD, FTIR, SEM/EDX, and UV-Vis spectroscopy.
- Environmental Application: A rigorous assessment of the nanoparticles' effectiveness in photo-degradation activity, with a focus on the elimination of contaminants and organic dyes from wastewater when exposed to visible light.

This work aims to bridge the gap between traditional botany, Chemistry and advanced materials science, offering a "green" solution to the growing global challenge of water pollution.

- Authors

Mr. Rahul Kumar

Dr. Bassa Satyannarayana

ACKNOWLEDGEMENT

I would like to express my deep sense of gratitude to my guide of Prof. (Dr.) Bassa Satyannarayana, Assistant Professor, Department of Chemistry, Govt. M.G.M. P.G. College, Itarsi, Madhya Pradesh. Who guided me to carry out this project successfully and has been a constant source of inspiration and strength to me throughout my study. I had a wonderful experience of working with him as she has tried his best in providing me every kind of support.

I remain indebted to my parents who have a shower of blessing of me starting from my inception of the project till the very end.

Last but not least, I would like to express my gratitude to all who directly or indirectly helped me to accomplish this project report.

- Author

Mr. Rahul Kumar

TABLE OF CONTENT

LIST OF TABLES

LIST OF FIGURES

ABSTRACT:

The development of environmentally friendly methods for synthesizing Nano materials has gained significant attention in recent years. In this work, Nano-ferrite particles were synthesized using green synthesis approaches, employing aqueous leaf extract of various plants such as Mango, Eucalyptus, and Neem as reducing and stabilizing agents. The biosynthesized ferrite nanoparticles were systematically characterized to evaluate their structural, morphological, and magnetic properties using standard analytical techniques. Structural analyses confirmed the formation of crystalline ferrite phases, while morphological studies revealed uniform distribution and Nano scale dimensions. Magnetic measurements demonstrated their potential as functional magnetic materials. Furthermore, the photo catalytic performance of the synthesized particles was investigated, highlighting their effectiveness in environmental remediation applications. This study underscores the potential of plant-mediated synthesis as a sustainable and cost-effective route for producing ferrite nanoparticles with dual functionalities in magnetic and photo catalytic domains.

KEYWORDS:

Green Synthesis, Nano-Ferrite Particles, Photo Catalytic, Biosynthesized, XRD, SEM, FTIR, UV-Visible Spectroscopy.

CHAPTER 1
INTRODUCTION

1.0. NANOTECHNOLOGY

Advances in technology and human living standards are tightly linked to advances in materials and how they are made. Traditional processing methods usually start from large pieces and cut, press, or deform them into the required shape. This often introduces strain, lattice defects, and other imperfections in the material. At the Nano scale, however, materials behave differently because their properties are strongly affected by size and surface effects, giving rise to new "quantum size" behaviors that can be used in future devices.

Nanoparticles [1] are extremely small; even a single particle may contain only a few to a few tens of atoms or molecules. At this scale, defects created by rough mechanical processing cannot simply be averaged out, and conventional methods also struggle to produce particles with a narrow and well-controlled size range. Therefore, nanoparticles are typically prepared using chemical routes. One common approach is to dissolve suitable precursors in a solution and then trigger a controlled precipitation reaction so that tiny particles form directly. Another route is to create a micro emulsion: two immiscible liquids (such as oil and water) are mixed with surfactants, forming tiny droplets (micelles) that confine the reactants. Nanoparticles then grow inside these droplets, giving a colloidal suspension.

However, these nanoparticles tend to attract each other through van der Waals forces and other thermodynamic driving forces. Over time, they stick together, grow larger, and eventually settle out of the liquid. For applications, it is essential to keep them dispersed and stable in the colloid. Two main strategies are used for stabilization. In electrostatic stabilization, ions are adsorbed on the nanoparticle surface, building an electrical double layer. When two particles approach, this like-charge repulsion prevents them from coming close enough to aggregate. In steric stabilization, polymer chains are attached or adsorbed on the surface of the nanoparticles. When two coated particles approach each other, the compressed polymer layers experience an osmotic and entropic repulsion, which keeps the particles separated and stops them from clumping together.

Nano crystalline spinel ferrites are technologically important because of their wide applications, and it is believed that the production of ferrites will increase year by year as their applications become more and more diverse. Even though the saturation magnetization of ferrites is less than half of ferromagnetic alloys. Nano ferrite materials are magnetic nanomaterial with a spinel crystal structure, generally represented by the formula AB_2O_4. In this formula, A and B refer to different metal ions such as iron, cobalt, nickel, zinc, or manganese. Due to their tiny size and

precisely arranged crystal lattice, these materials exhibit distinctive magnetic, electrical, and catalytic behaviors. The most important advantage of ferrites is their very high degree of compositional variability. Most of the original intrinsic properties on ferrites are made on the simple ferrites such as $MnFe_2O_4$, $CoFe_2O_4$, $NiFe_2O_4$ and $CuFe_2O_4$. Distribution of cations over A and B sites has a profound effect on the electricaland magnetic properties of spinel ferrites. The properties of Nano ferrites are influenced by the composition and microstructure, which are sensitive to the preparation methodology used in the synthesis and to the sintering conditions. Ferrite nanoparticles are usually prepared by various physical and chemical methods

1.1. PROCESSING METHODS

Nanostructure materials are single phase or multiphase polycrystalline solids with a typical average size of a few nanometers (1nm = 10-9m). Basically, the range from (1-100) nm is taken as Nano-range for convention. The synthesis of nanomaterial can be well accomplished by two approaches. Firstly, by “Bottom Up” method where small building blocks are produced and assembled into larger structures. Where the main controlling parameters are morphology, crystallinity, particle size, and chemical composition. Examples: chemical synthesis, laser trapping, self-assembly, colloidal aggregation, etc and secondly, by “Top Down” method where large objects are modified to give smaller features. For example: film deposition and growth, Nano imprint/lithography, etching technology, mechanical polishing etc. The main reason of alteration in different mechanical, thermal and other property is due to increase in surface to volume ratio. Synthesis of nanomaterial is most commonly done based on three strategies i.e.

- Liquid-phase Synthesis.
- Gas-phase Synthesis.
- Vapor-phase Synthesis.

A. liquid-phase Synthesis

Under liquid phase synthesis the techniques used for synthesis are:

- Co-precipitation.
- Sol-gel Processing.
- Micro-emulsions.
- Hydrothermal/Solvo-thermal Synthesis.
- Microwave Synthesis.
- Sono-chemical Synthesis.
- Template Synthesis.

B. Gas-Phase Synthesis

- Super saturation achieved by vaporizing material into a background gas, then cooling the gas.

C. Methods using solid precursors

- Inert Gas Condensation
- Pulsed Laser Ablation
- Spark Discharge Generation
- Ion Sputtering

D. Methods using liquid or vapor precursors

- Chemical Vapor Synthesis
- Spray Pyrolysis
- Laser Pyrolysis/ Photochemical Synthesis
- Thermal Plasma Synthesis
- Flame Synthesis
- Flame Spray Pyrolysis
- Low-Temperature Reactive Synthesis

Nano structured materials can have significantly different properties, depending on the chosen fabrication route. Each method offers some advantages over other techniques while suffering limitation from the others. [2]

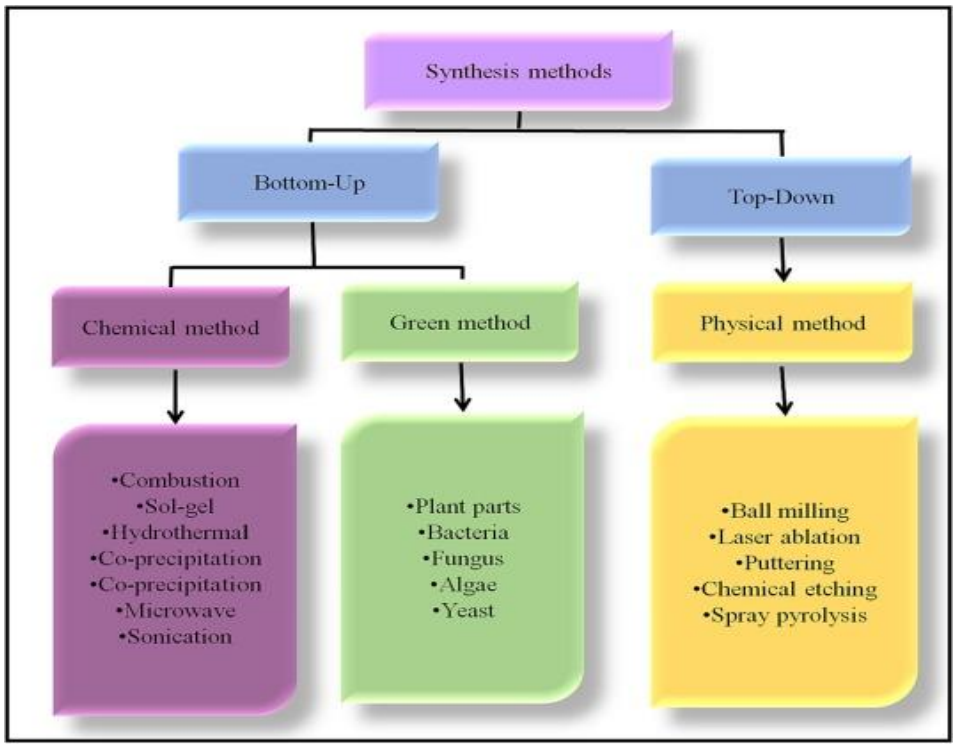

Figure 1.1: Flow chart of Synthesis Methods

1.2. FERRITES

Ferrites are ceramic compounds composed of iron oxide (Fe_2O_3) combined with other metallic elements. Electrically, ferrites are non-conducting materials. Ferrites are the most important ferrimagnetic substances which contains certain oxides of iron (Fe) and another metal. The general forms of ferrites are mostly ionic in nature and are stable in their crystalline structure due their oxide bonding that exists between the metal ions. Some ferrites are based on Mn, Cr and other elements, but in most of the ferrites, iron oxide (either Fe_2O_3 or Fe_3O_4) would be a major component. In electronic transformers, inductors and electromagnets, the cores of ferrites are used in which they exhibit very low eddy current losses and have high electrical resistance. In data cable, ferrite beads are used as a lump which helps to resist the electrical noise of high frequency. [3]

1.3. CLASSIFICATION OF FERRITES

- On the basis of hysteresis, and the characteristics of ferrite they are classified as hard or soft magnetic materials.
- On the basis of structure, these are classified as spinel ferrites, garnets, ortho ferrites and hexagonal ferrites.

1.3.1. On the basis of Hysteresis

Ferrites are classified on the basis of the hysteresis loop broadening such as:

- **Soft ferrites**

Soft ferrites can be easily magnetized by exposing them in an applied magnetic field environment and it is reverted to the nonmagnetic state when the field is removed. Good examples of soft ferrites are manganese ferrite, nickel ferrite, zinc ferrite and the various compositions of these mixed ferrites (Mn-ferrite, Mn-Zn ferrite and Ni- Zn ferrite).

Ferrites are widely used in transformers or cores that contain metals such as zinc, nickel, zinc or manganese based mixed compounds which usually possess low coercivity are classified under the category of soft ferrites. They find extensive use in radio frequency (RF) transformers, Switched-Mode Power Supply (SMPS) and in inductor coils due their lower losses at higher frequencies.

According to site preference, soft ferrites can be classified as:

- Normal spinel ferrite
- Inverse spinel ferrite
- Mixed spinel ferrite

Normal spinel ferrite

In a normal spinel ferrite, the trivalent ions occupy the octahedral sites and the divalent metal ions occupy the tetrahedral position. Examples of spinel ferrites are zinc ferrite ($ZnFe_2O_4$) and cadmium ferrite ($CdFe_2O_4$).

Spinel structure

The unit cell of the spinel has eight formula units (8 x AB_2O_4) in which there are 32 oxygen ions which forms a face centered cubic (FCC) lattice. There are two interstitial sites namely tetrahedral sites (A sites) and octahedral sites (B sites) Typical ratio is A: B: O= 8:16:32 the crystal structure of a spinel ferrite is shown in Figure 1.2 consists of unit cells with edge a/2 where "a" is the edge of the unit cell as eight ants. All the octant positions are occupied by the oxygen atom and that the location of the oxygen ions and metal ions can be easily identified from the figure1.2.

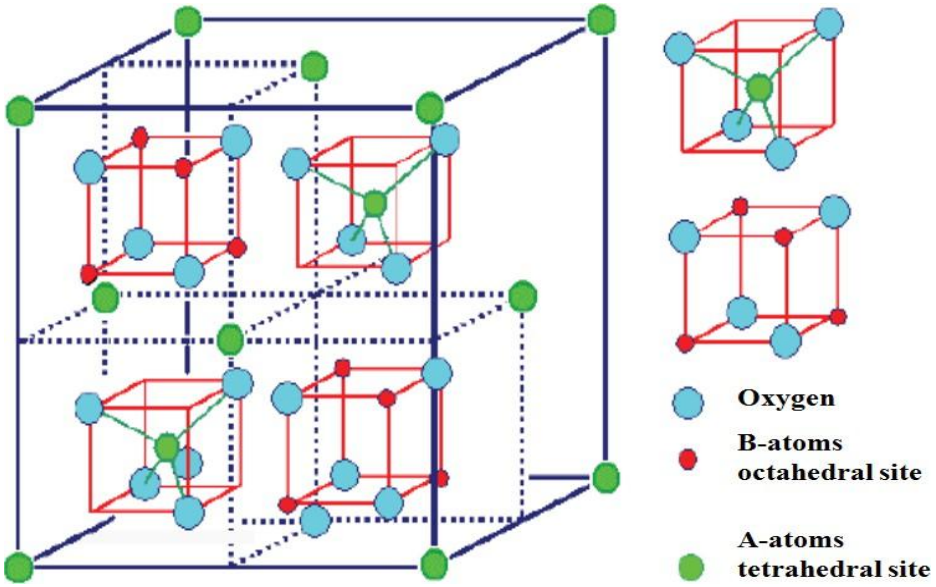

Figure 1.2: Structure of spinel (AB_2O_4)

Inverse spinel ferrite

In an inverse spinel, the distribution is flipped

- B cations split between tetrahedral and octahedral sites
- A cations occupy only octahedral sites
- For example, in cobalt ferrite ($CoFe_2O_4$) nickel ferrite ($NiFe_2O_4$).
- Co^{2+} occupies octahedral sites
- Fe^{3+} splits between tetrahedral and octahedral sites.

Mixed spinel ferrite

Many ferrites consists of both normal and inverse spinels and thereby exists an intermediate phase are termed as mixed spinel ferrites. Examples of such mixed spinel ferrite are nickel ferrite

($NiFe_2O_4$) which consists of 80 % inverse spinel and 20 % of normal spinel, and $MnFe_2O_4$ which has 20 % inverse spinel and 80 % of normal spinel structures.

Hard ferrites

Hard ferrites retain their magnetization as long as there is no counter-magnetizing field with sufficient strength to annihilate or to reverse the state of alignment.

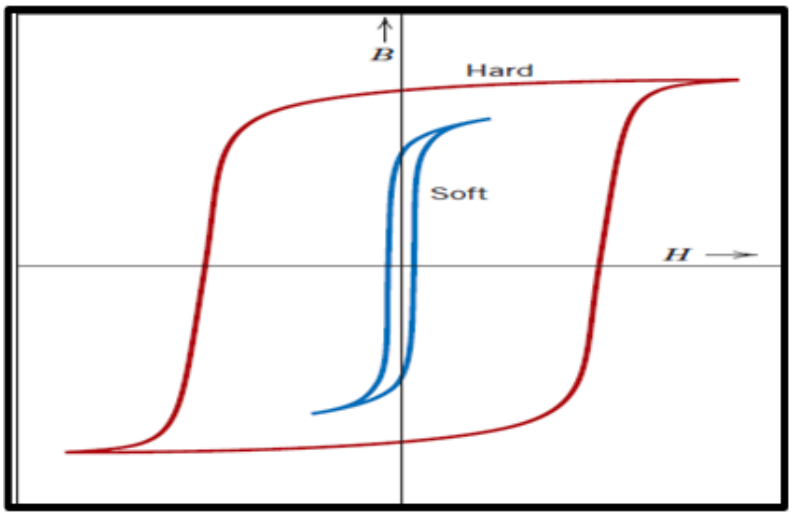

Figure 1.3: Hysteresis of ferrites

Figure 1.3 shows that hard ferrite is readily distinguished by its broad hysteresis loop from the soft ferrite, indicating a high coercive field. Barium ferrite [$Ba_{0.6}Fe_2O_3$] and Strontium ferrite [$Sr_{0.6}Fe_2O_3$] are the most widely used hard ferrites at present in many industrial applications on a large scale. There are certain ferrites termed as "hard ferrites" possess high remanence and coercivity after magnetization is also called as permanent magnetic ferrites. Normally strontium and barium based ferrites possess high magnetic permeability finds applications in magnets in radios. In computer cable, a lump can be seen are termed as “ferrite bead” which possess low eddy current helps us to prevent from noises due to high frequency in cables. It also finds applications in radar component for absorbing materials and also as coatings in aircraft applications in rooms to prevent electromagnetic interferences.

1.3.2. On the basis of structure

Depending upon the crystal structure, they can be classified as:

- Ferro spinels
- Garnets
- Orthogonal Ferrites
- Hexagonal Ferrites

Ferro spinels

Ferro spinels shown in Figure 1.4 have the molecular formula MFe_2O_4, in which "M" is a divalent transition metal ion like Mn, Co, Zn, Ni, etc. with a valence of 2 or a mixture of divalent transition ions with a valence of 2. Oxygen ion forms a closely packed FCC structure in which the metal ions occupy tetrahedral and octahedral sites. The four (4) oxygen ions are surrounded in the tetrahedral sites and six (6) oxygen ions occupy at the octahedral sites.

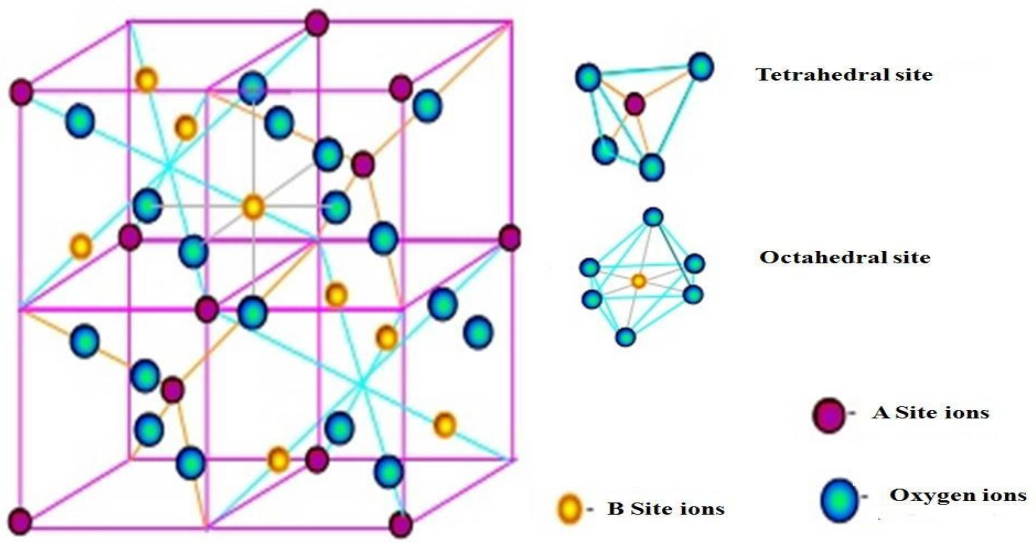

Figure 1.4: Ferro spinel structure

In a unit cell, only 8 sites are occupied out of 32 sites and 16 sites are occupied out of the 64 available tetrahedral sites. Manganese- zinc ferrite ($Mn_xZn_{(1-x)}Fe_2O_4$) is one such spinel ferrite shown in above Figure 1.4 is a class of Ferro spinel structure belonging to the soft ferrites group.

Garnets

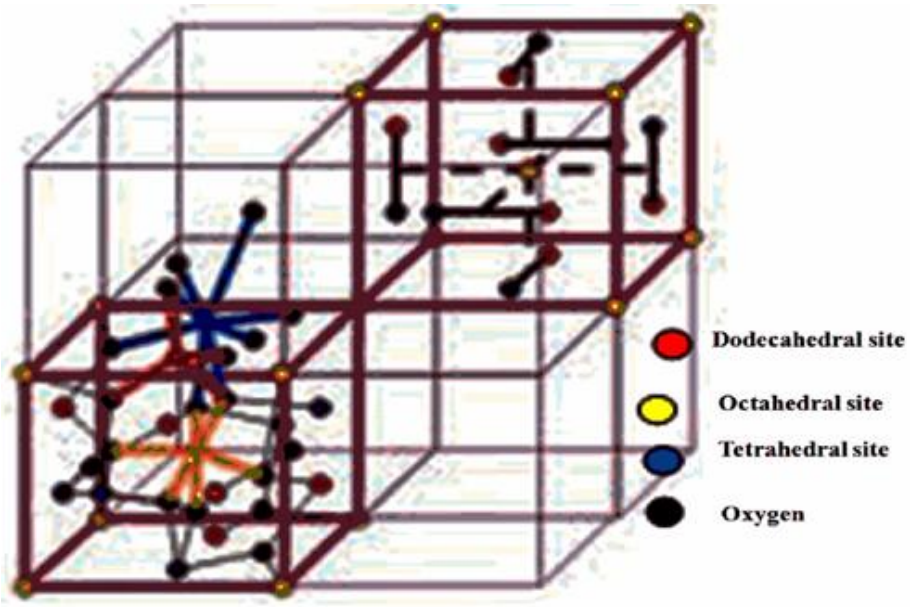

Figure 1.5: Crystal structure of garnet

Garnets have the general formula $M_3Fe_5O_{12}$ where, M is a trivalent ion such as rare-earth. The unit cell is cubic and contains eight molecules of $M_3Fe_5O_{12}$. Apart from the tetrahedral and octahedral sites present in spinels, garnets possess dodecahedral sites with 12- coordinated. Among the three sites available with anti-parallel spin, the ferrimagnetism structure is shown in below Figure 1.5 in which all the oxygen, metal and ferrite ions are represented in different colors.

These types of garnets consists of more complex structures in which there are 24 (yttrium) Y^{3+} in dodecahedral site and 24 (ferrite) Fe^{3+} ions in the tetrahedral sites whereas the remaining 16 sites are occupied by Fe^{3+} ions in the octahedral sites. There are numerous transition metals available in which either ferrite or yttrium itself can be replace by some of rare earth ions in the octahedral and dodecahedral sites. These garnets find much application such as microwaves which are usually at very high frequencies

Ortho Ferrites

Ortho ferrites have the molecular formula $MFeO_3$, in which "M" is a trivalent ion such as rare-earth. Figure 1.6 shows that they crystallize in a distorted perovskites structure with an orthorhombic unit cell. They are used for bubble domains. Ortho ferrites belong to a space group pbnm and most of them are weakly ferromagnetic.

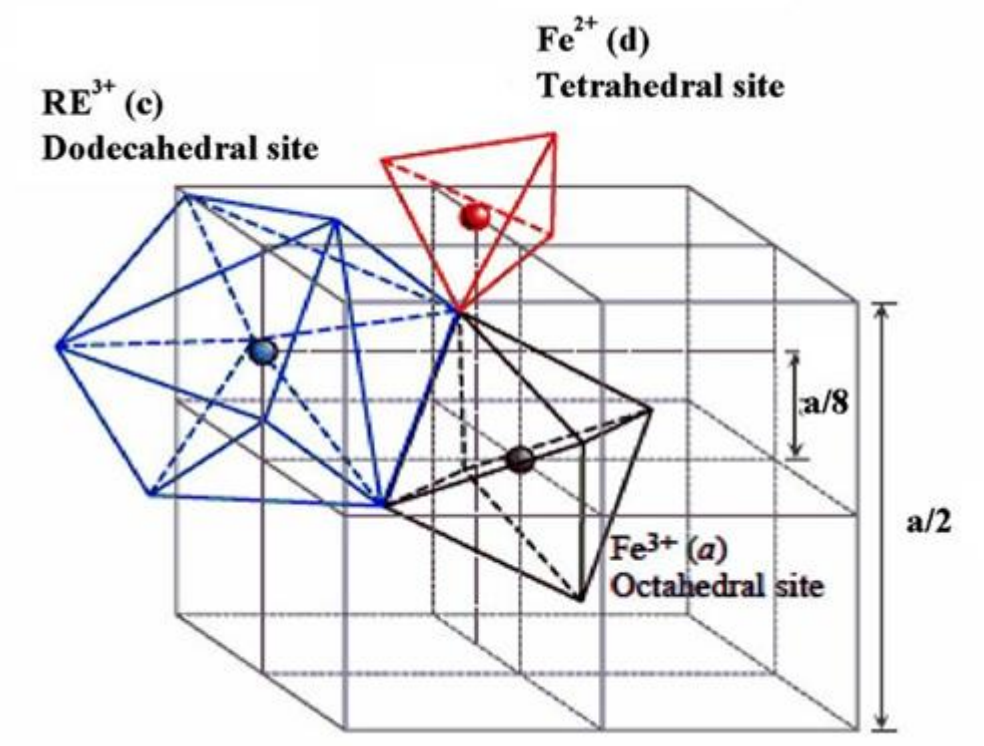

Figure 1.6: Structure of ortho ferrite

Hexagonal Ferrites

Hexagonal Ferrites have the molecular formula $MFe_{12}O_{19}$ in which "M" is a divalent metal ion with large atomic radius which crystallizes in hexagonal structure and that there were several metals such as strontium (Sr), barium (Ba) and lead (Pb) were widely used as metal replacements to suit the parent atomic radii.

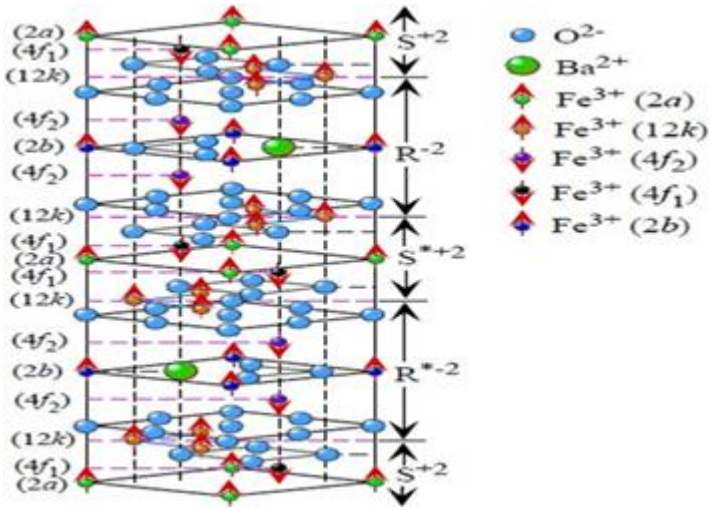

Figure 1.7: Hexagonal structure of ferrites

The hexagonal structure in the ferrites is shown in above Figure 1.7 in which the presence of unique 'c' axis or vertical axis along which magnetization occurs and thus this direction cannot be changed in these types of ferrites and hence are termed as "hard ferrites". They find numerous applications due to their magneto-crystalline anisotropy and also higher saturation magnetization. By varying the chemical composition of these hexagonal ferrites they magnetic properties can be tuned and also by varying the particle size its properties can be modified.

1.4. PHOTO CATALYTIC DEGRADATION

The wastewater discharged from textile and dyestuff industries cause serious environmental problems by destroying various life forms and consume dissolved oxygen owing to its strong color, a large amount of suspended solids, highly fluctuating pH as well as high temperature. Synthetic dyes are generally used in numerous manufacturing industries such as paper printing, textile dyeing cosmetics and pharmaceuticals. About 15–20% of the total world production of dyes is lost during the dyeing processes.

Methylene Blue, Rhodamine B is widely used in industrial purposes and capable to cause irritation to the skin, eyes, gastrointestinal tract as well as respiratory tract. Therefore, treatment of dye-containing effluents, i.e. Rhodamine B and Methylene Blue is a topic of significant interest among researchers. Color is one of the vital characteristics of these effluent streams and seems to be the most undesired, as it affects the nature of water by inhibiting sunlight penetration

hence reducing photosynthetic action. Thus, color removal from industrial effluents has become a major concern in wastewater treatment, and treatment is needed before discharging to receiving water. For the removal of dye pollutants, various conventional methods such as adsorption on activated carbon, ultra filtration, reverse osmosis, coagulation by chemical agent etc. can generally be used efficiently. Nevertheless, they are nondestructive methods, since they just transfer organic compounds from waste water to another phase, thus causing secondary pollution easily. Due to the large numbers of aromatic compounds present in dye molecules and stability of modern dye, the conventional treatment Contamination of water and air due to organic matter possesses severe threat to life on the earth. The presence of such matter increases the environmental pollution. Degradation of such pollutants becomes the need of the hour to minimize the pollution. Use of semiconductors for photo catalytic activity has attracted attention as they potentially degrade the organic pollutants in water and air. Irrespective of the types and activities of semiconductors, photo catalytic reactions can work at ambient conditions, without producing any additional pollutant**.** The general scheme for the photo catalytic destruction of organic compounds involves the following three steps:

i. When the energy hυ of a photon is equal to or higher than the band gap (Eg) of the semiconductor, an electron is excited to conduction band, with simultaneous generation of a hole in the valance band.
ii. Then the photo excited electrons and holes can be trapped by the oxygen and surface hydroxyl, respectively, and ultimately produce the hydroxyl radicals (•OH), which are known as the primary oxidizing species; and methods are ineffective for decolonization and mineralization.
iii. The hydroxyl radicals commonly mineralize the adsorbed organic substances.

Among various semiconductor photocatalysts, Nano ferrites (MFe_2O_4), where M is a divalent metal such as Ni, Co, Cu, or Zn) have emerged as an important class of materials because they combine good photo catalytic activity with chemical and photo stability. Nano ferrites possess tunable band gaps and magnetic properties, which facilitate efficient charge separation and easy recovery of the catalyst from treated water. Compared with many traditional oxides, suitably engineered ferrite nanostructures can absorb a significant portion of the visible as well as UV region, making them attractive for solar-driven degradation of organic pollutants. Key limitation in semiconductor photocatalysis is the recombination of photo-generated electron–hole pairs, which suppresses overall activity. In Nano ferrites, this drawback can be mitigated by tailoring cation distribution, particle size, and morphology or by incorporating additional metals and forming ferrite-based composites and hetero junctions that promote charge separation.

Methylene Blue (MB) and Rhodamine B (RB) are common water-soluble dyes extensively used in textile, printing, paper, pharmaceutical, and food industries, and they are often chosen as model pollutants for evaluating ferrite photocatalysts. In a typical study, nano ferrite catalysts are employed to drive the photodegradation of MB and RB under light irradiation, and the degradation efficiency can be further enhanced by the controlled generation of hydroxyl radicals using suitable oxidants such as hydrogen peroxide, which act synergistically with the ferrite surface to mineralize the dyes more effectively.

1.5. PHOTO CATALYST

Photo-Catalysis defined as "acceleration by the presence of as catalyst". A catalyst does not change in itself or being consumed in the chemical reaction. This definition includes photosensitization, a process by which a photochemical alteration occurs in one molecular entity a result of initial absorption of radiation by another molecular entity called the photosensitized. Chlorophyll of plants is a type of photo catalyst. Photo catalysis compared to photosynthesis, in which chlorophyll captures sunlight to turn water and carbon dioxide into oxygen and glucose, photo catalysis creates strong oxidation agent to breakdown any organic matter to carbon dioxide and water in the presence of photo catalyst, light and water.

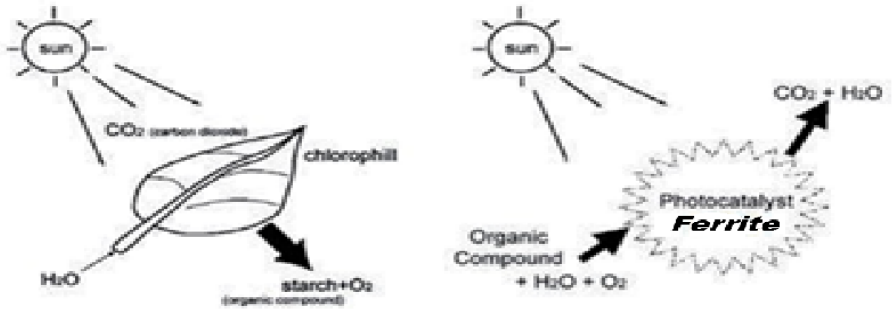

Figure 1.8: Photo catalysis Mechanism

1.5.1. Mechanism

Photo-excitation of ferrite

When a ferrite semiconductor absorbs light with photon energy equal to or greater than its band-gap energy, electrons in the valence band (VB) become excited and are promoted to the conduction band (CB). The promotion of these electrons leaves behind positively charged holes in the VB, producing electron–hole pairs (e^-/h^+). This light-induced generation of charge carriers is called the photo-excited state of the ferrite semiconductor.

Band gap and excitation wavelength

The energy separation between the VB and CB is the band gap of the ferrite. For many spinel ferrites this band gap lies roughly in the range 1.5–2.5 eV, so the required excitation wavelength

typically falls in the visible to near-UV region, which can be estimated with λ (nm) ≈1240/Eg (eV) λ (nm) ≈1240/Eg (eV). For example, a ferrite with Eg=2.0 eV, Eg=2.0 eV will be photo-excited by light of wavelength around 620 nm or shorter.

Redox reactions at the surface

Once generated, CB electrons migrate to the ferrite surface, where they can reduce dissolved oxygen molecules to superoxide radicals (O2·−O2·−). At the same time, VB holes move to the surface and oxidize surface hydroxyl groups or adsorbed water to produce highly reactive hydroxyl radicals (·OH·OH). These reactive oxygen species, together with the holes themselves, attack and decompose organic pollutants, dyes, or microorganisms adsorbed on the ferrite surface.

Photo catalytic cycle of ferrite

As long as light with sufficient energy continues to irradiate the ferrite, new electron–hole pairs are generated and the redox cycle repeats. Efficient photo catalytic activity depends on three main factors: effective absorption of the incident light, rapid separation and transport of the electron–hole pairs, and a high density of active surface sites where redox reactions can occur. Tailoring cation composition, particle size, and morphology of ferrites is a common strategy to minimize charge recombination and enhance this repeating photo catalytic cycle.

1.6. MINERAL ANALYSIS OF LEAF POWDERS

For my project work, I use three sample powders—moringa, mango, and Neem—for the green synthesis of Nano ferrites. To understand which key minerals are present in these powders, I conducted a comprehensive literature review of various articles. Based on this review, I prepared a detailed table listing the minerals detected in these leaf powders. Most researchers employ advanced analytical techniques such as Energy Dispersive X-ray Analysis (EDAX) and X-ray Photoelectron Spectroscopy (XPS) to quantify the elemental composition and concentration in these samples. This mineral profiling is crucial for guiding further experimental work and optimizing the green synthesis process of ferrite nanoparticles.

1.7. MORINGA

Moringa tree, scientifically known as Moringa oleifera, is a fast-growing, drought-resistant tree belonging to the family Moringaceae. It is native to northern India and widely found across tropical and subtropical regions of India. Commonly called the drumstick tree due to its long, slender seed pods, it thrives in dry and moist deciduous forests and is extensively used for its nutritious leaves, pods, and medicinal properties.

Moringa leaf powder has gained considerable attention as a natural and eco-friendly resource for the green synthesis of ferrite nanoparticles. Due to its rich content of bioactive compounds, including polyphenols, flavonoids, and Reducing agents, Moringa leaf powder is an excellent

green precursor for the synthesis of functional ferrite nanoparticles, offering a sustainable, cost-effective and scalable approach. This eco-friendly synthesis route bridges plant-based chemistry and nanotechnology for future scientific innovations researchers employ advanced analytical techniques as Energy Dispersive X-ray Analysis (EDAX) and X-ray Photoelectron Spectroscopy (XPS) to quantify the elemental composition and concentration in these samples. [4]

Figure 1.9: Moringa powder

The study work is used for Elemental analysis of moringa leave powder [4] and this emphasizes 13 essential elements, namely, Na, K, Ca, Mg, Cr, Mn, Fe, Co, Ni, Cu, Zn, Sr, and B, are found in leaves powder and findings are presented in Table 1.1

Table 1.1: Mineral composition of Moringa leaf [4]

Sl. No.	Element	Concentration (mg/kg)
1	Boron (B)	31.68
2	Calcium (Ca)	6767.79
3	Cobalt (Co)	Not observed
4	Chromium (Cr)	3.01
5	Copper (Cu)	0.09
6	Iron (Fe)	21.88
7	Potassium (K)	10,500.08
8	Magnesium (Mg)	32.80
9	Manganese (Mn)	45.91
10	Sodium (Na)	1498.46
11	Nickel (Ni)	1.23
12	Strontium (Sr)	27.87
13	Zinc (Zn)	33.87

1.8. NEEM

The Neem tree, scientifically known as *Azadirachta indica* [5], is a fast-growing, evergreen tree belonging to the mahogany family, Meliaceae. Native to the Indian subcontinent, it usually reaches a height of 15-20 meters but can grow taller under favourable conditions. Known for its wide-ranging medicinal and agricultural uses, Neem is often called the "Free Tree of India." It thrives in tropical and subtropical climates and is valued for its leaves, seeds, and bark, which contain bioactive compounds with insecticidal and therapeutic properties. Neem plays a vital role in traditional medicine, pest control, and environmental sustainability. Neem leaves powder is widely recognized for its bioactive compounds and medicinal properties. Elemental analysis of Neem leaf powder by EDX-7000 spectrometer [6] reveals the presence of elements shown in table 1.2.

Figure 1.10: Neem powder

Table 1.2: Elemental Concentration in Neem Leaves Sample [6]

Sr. No.	Element	Concentration (%)
1	Ca	1.314
2	K	0.842
3	S	0.114
4	Sr	0.011
5	Fe	0.008
6	Cu	0.002
7	Ti	0.002
8	Mn	0.001
9	Br	0.001
10	Zn	0.001
11	Rb	0.001

These elements contribute to Neem's nutritional, pharmaceutical, and material science applications, particularly in green synthesis processes similar to those using moringa leaf powder. Such elemental richness supports Neem's use as a natural reducing and stabilizing agent in eco-friendly nanoparticle synthesis, including ferrites. This elemental profile is instrumental for research in green chemistry and sustainable materials development.

1.9. MANGO

The Mango tree (Mangifera indica) is a large, evergreen tropical tree commonly found in India and many tropical regions worldwide. It can grow up to 30-40 meters tall and is highly valued for its delicious fruit. The tree has dark green, lance-shaped leaves and produces small, fragrant flowers in large clusters.

In recent research, mango leaf powder has been used as a green reducing and stabilizing agent for the synthesis of ferrite nanoparticles, particularly magnetite (Fe_3O_4). The phytochemicals in mango leaves, including polyphenols and flavonoids, facilitate the reduction of metal salts to Nano sized ferrites and prevent agglomeration, resulting in stable, high-surface-area nanoparticles. These green-synthesized ferrites have applications in environmental remediation, catalysis, and magnetic materials due to their eco-friendly production and functional properties. Thus, mango leaf powder serves as a sustainable and effective natural precursor for ferrite nanoparticle synthesis, combining plant-based chemistry with advanced nanotechnology.

Elemental analysis of mango leaf powder reveals the presence of minerals such as potassium (K), calcium (Ca), magnesium (Mg), iron (Fe), sodium (Na), zinc (Zn), manganese (Mn), and copper (Cu). These elements contribute to the nutritional and Bioactive properties of mango leave [7].

Figure 1.11: Sample of Mango powder used for Synthesis

Table 1.3: Elemental Concentration of Dried Mango Leaves [7]

Element	Symbol	Concentration Range
Potassium	K	368–589 mg
Phosphorus	P	0.007–0.48 % (≈ 480 mg)
Calcium	Ca	0.003–4.41 %
Magnesium	Mg	0.009–1.58 %
Iron	Fe	0.0062–0.034 %
Zinc	Zn	0.0024–0.014 %
Sodium	Na	0.003–0.23 %
Copper	Cu	0.0021–0.0029 %
Manganese	Mn	0.0028–0.003 %
Nitrogen	N	0.003–2.6 %
Cadmium	Cd	Trace (~0.015 %)

CHAPTER 2
LITERATURE REVIEW

2.1 LITERATURE

S. Dichayal, *et al.* (2024): This University Journal is related to how plants and their extracts are increasingly being used to synthesize cobalt ferrite nanoparticles. These natural materials act as reducing and capping agents, helping produce nanoparticles with controlled properties. The review also covers the different techniques used to study the structure, shape, and magnetic features of these nanoparticles, as well as their many practical uses. Cobalt ferrite nanoparticles ($CoFe_2O_4$) have become highly popular because they're used in so many different fields, from medicine and environmental cleanup to energy devices and various industrial applications. Lately, there's been a shift toward greener ways of making these nanoparticles, since traditional chemical and physical methods can cause environmental harm. Green methods are not only cost-effective but also safe and environmentally friendly. [8]

Nur D Zambri, *et al.* (2019): In this Article, Green synthesis of magnetite nanoparticles using Neem leaf extract provides an eco-friendly approach compared to conventional synthesis routes. Characterization studies confirm their nanoscale dimensions, purity, and super paramagnetic behavior, which make them suitable for targeted drug delivery and other biomedical uses. This work demonstrates how plant-based synthesis offers a sustainable pathway for developing functional ferrite nanoparticles with promising applications. [9]

Tejashwini *et al.* (2024): In this research work highlights that industrial dyes severely contaminate water sources, posing serious risks to aquatic life. Among emerging solutions, Nano ferrites stand out as efficient photo catalytic materials due to their narrow band gap, chemical stability, high porosity, effective separation of charge carriers, and magnetic properties that facilitate recovery. These features make ferrites highly suitable photocatalysts for wastewater treatment. Photocatalysis is an environmentally friendly and straightforward process, is increasingly recognized for its effectiveness in degrading industrial dyes using specially engineered nanoparticles. Importantly, it also demonstrates how ferrites synthesized via both chemical and green approaches. Ultimately it supporting improved environmental monitoring and the pursuit of zero energy waste systems. [10]

Alqassem B *et al.* (2024): This review explores another way to enhance properties of Nano ferrite particle by combined with advanced materials, such as BiOX, MXene, and g-C_3N_4 to form binary and ternary nanocomposites. These ferrite nanocomposites showed superior Photocatalytic performance due to enhanced properties such as increasing the capacity for light utilization, slowing electron-hole recombination, and reducing agglomeration and to fine-tune morphology and enhance catalytic efficiency**.** [11]

Shelash S. I. *et al.* (2025): This review explores the combination of Nano ferrites with the clay mineral montmorillonite (MMT) to enhance performance. The MMT/$CuFe_2O_4$ Nano composite acts as a strong, reusable, and safe photocatalyst. It performs well in removing dyes and cleaning the environment under both UV and visible light due to the combined effects of MMT's dye adsorption and $CuFe_2O_4$ Photocatalytic activity. Montmorillonite is layered clay with a large surface area and ion exchange ability, allowing it to capture dye molecules and bring pollutants close to the catalyst. $CuFe_2O_4$, a spinel ferrite with a narrow band gap (about 1.6–2.1 eV), absorbs visible light effectively. When light hits it, it creates charged particles (electron-hole pairs) that generate reactive oxygen species like hydroxyl and superoxide radicals. These species break down dye molecules into harmless substances such as carbon dioxide and water. [12]

Sidhaarth, A. K. R. *et al.* (2015): The present study has examined the adsorption of Lead, Zinc and Congo red dye from synthetic wastewater using cobalt ferrite nanoparticles and manganese ferrite nanoparticles. The purpose of selecting the nanoparticles is because of its unique property of having higher surface area per unit volume and this factor plays a critical role in the adsorption practices. The nanoparticles were synthesized by co-precipitation method**.** [13]

K. Swapna *et al.* (2011): A simple and efficient procedure for the synthesis of diaryl selenides has been developed by a copper ferrite nanoparticle catalyzed. The copper ferrite nanoparticles were magnetically separated, recycled, and reused up to three cycles.[14]

Satyanarayana Bassa *et al.* (2016): This study work shows a simple, multi component, one-pot method for the synthesis of poly substituted imidazoles in presence of magnetically separable and recyclable spinel Nano copper ferrite as heterogeneous catalyst. It means these particles also help synthesis of other compounds. [15]

Singh, S. *et al.* (2021): This work clearly shows that spinel Nano ferrites are attractive materials for wastewater treatment because they are stable, easy to synthesize, magnetically separable, and can be easily modified. While many studies have explored doping as a way to improve their properties, there is still limited understanding of how different metal ions specifically affect their catalytic behavior. In addition, research on ternary composites and more complex heterostructures of spinel Nano ferrites for removing stubborn pollutants is still in its early stages. Therefore, future studies should focus on a more systematic design of doped and surface-functionalized spinel Nano ferrites, including their combination with carbon-based materials or polymers, to improve catalytic performance while preserving simple magnetic recovery and overall cost-effectiveness**.** [16]

Aji Udhaya, P. (2021): The literature shows that nanosized spinel oxides are highly promising materials because their electrical, magnetic, catalytic, and electrochemical properties improve

significantly at the nanoscale. Chemical synthesis methods such as co-precipitation and auto-combustion allow good control over particle size and morphology without introducing impurities. Spinel oxides like Co_3O_4, $CoFe_2O_4$, $ZnFe_2O_4$, and Fe_3O_4/γ-Fe_2O_3 have demonstrated strong potential in applications ranging from gas sensing and catalysis to energy storage and magnetic devices. Overall, these studies emphasize that controlled synthesis plays a key role in tailoring material properties for advanced applications**.** [17]

Sunny, A. (2020): Magnetic hyperthermia therapy offers new hope as a complementary cancer treatment by using magnetic nanoparticles to generate heat that selectively kills tumor cells at temperatures between 42-46°C. While iron oxide nanoparticles have been explored for this purpose, they fall short in heating efficiency and have Curie temperatures that are too high for safe therapeutic use. This research tackled these problems by developing spinel ferrite nanoparticles (MFe_2O_4, where M = Co, Ni, Mg, Zn) through straightforward synthesis methods. By carefully adjusting the amount of zinc in these nanoparticles, researchers were able to fine-tune the Curie temperature to stay below 46°C, which helps prevent overheating and protects healthy tissue from damage. The nanoparticles created in this study showed all the key qualities needed for effective hyperthermia treatment: they were uniform in size, stable in the body, biocompatible, and produced heat efficiently. These results show that specially designed spinel ferrite nanoparticles work better than traditional iron oxide nanoparticles and provide a safer, more effective option for treating cancer with magnetic hyperthermia**.** [18]

Hariganesh, S. (2021): This research work focused on developing visible-light-responsive photocatalysts for the degradation of organic pollutants and dyes present in industrial effluents. While conventional photocatalysts such as TiO_2 and ZnO are widely used, copper-based materials like CuO and CuS have gained attention due to their strong visible-light absorption and reduced charge recombination. However, their practical application is limited by poor structural stability. To overcome these limitations, copper-based spinel and thiospinel systems have emerged as promising alternatives. These ternary transition-metal oxides and sulfides (AB_2X_4, X = O or S) exhibit enhanced optical, electrical, and magnetic properties owing to the presence of mixed oxidation states, which improve stability, electronic conductivity, and photo response. In particular, copper-based spinels and thiospinels such as $CuCr_2O_4$, $CuFe_2O_4$, and $CuCo_2S_4$ show significant potential for visible-light photocatalysis, though they remain underexplored. In this work, copper-based spinel and thiospinel nanocomposites were synthesized using a simple methodology and evaluated for their Photocatalytic efficiency in the removal of various pollutants under visible light. The synthesized composites were characterized using XRD, FT-IR, SEM, TEM, UV-DRS, and XPS to correlate their structural and chemical properties with Photocatalytic performance**.** [19]

Yadav, N., & Ahmaruzzaman, M. (2024): This study demonstrates that calcium ferrite ($CaFe_2O_4$) has strong potential for energy-related and environmental remediation applications. Its Photocatalytic activity is mainly attributed to its narrow band gap (~1.9 eV), high surface area, and effective pollutant degradation mechanisms. Although metal ferrites such as nickel, copper, zinc and cobalt ferrites are widely used as catalysts because of their abundance and versatility, calcium ferrite emerges as an excellent alternative. Being eco-friendly and non-toxic, $CaFe_2O_4$ also exhibits super paramagnetic behavior, which enables easy recovery from the reaction medium and enhances its practical applicability. Furthermore, this study highlights future perspectives for the development of sustainable $CaFe_2O_4$ and $CaFe_2O_4$-based nanocomposites with improved performance. [20]

2.2. OBJECTIVES OF THE WORK

- Introduction of Nano ferrite Particles.
- Synthesis of green Nano ferrites by using plant leaves of Moringa, Mango and Neem
- Characterization of synthesized Nano ferrite by using XRD, SEM, TEM, VSM (Vibrating Sample Magnetometer), BET (Surface Area.)
- Photo Catalytic study of synthesized Nano ferrite particle by photo degradation of some harmful dyes.
- Conclusion and Future scope.

Wastewater discharged from textile and dyestuff industries poses a major environmental challenge due to its intense color, which not only destroys aquatic life but also depletes dissolved oxygen levels. The strong coloration of these effluents significantly reduces light penetration, thereby inhibiting photosynthetic activity and disturbing the ecological balance of water bodies. Addressing this issue requires eco-friendly and sustainable treatment methods. Among the various approaches, photo catalytic degradation has emerged as a highly effective and green technique for treating dye-containing wastewater. In this work, an additional step toward sustainability is incorporated by synthesizing photo catalytic Nano Ferrite particles through green methods using plant leaf extracts as natural reducing and stabilizing agents. This eliminates the need for harmful chemicals, thereby minimizing secondary pollution. The work further evaluates the photo catalytic performance of the synthesized Ferrite particles and highlights their potential in environmental remediation applications.

CHAPTER 3
MATERIALS AND METHODS

3. EXPERIMENTAL WORK

Production of Nano ferrite particle in lab by leaves extracts. Using Co-precipitation Method.

3.1 SYNTHESIS OF GREEN FERRITE NANOPARTICLES

Among various synthesis methods for Nano ferrite particles, co-precipitation and sol-gel methods are generally considered the most cost-effective.

Co-precipitation: This method involves simultaneous precipitation of metal ions from solution by adding a precipitating agent (e.g., NaOH), forming ferrite nanoparticles. It requires relatively simple equipment, mild reaction conditions, and inexpensive precursors, making it one of the cheapest and scalable methods. It typically produces uniform particles with good crystallinity.

Nano ferrite has been produced from various plant components including flowers, leaves, shoots, seeds, fruits, and roots. A relatively simple Co-precipitation method is used for its biogenic production using only plant leaves. Plant leaves are collected from various sources and carefully cleaned with tap water and distilled water to remove any foreign impurities. Plant components are either used directly in the production of plant extracts or they are grind and dried to produce a powder. To extract the plant material, it is either cut into small pieces or grind into powder and then cooked in a mixture of water and ethanol at the correct temperature. The Nanoparticles synthesis can be done by using plant extracts and different concentrations as metal precursors. In brief, a solution of metal salt is combined with plant extract and the phytoconstituents in the extract serve as both a stabilizing and reducing agent for the production of ferrite. The addition of stabilizers or external chemical reducing agents is not necessary. The next step to separate the NMs is to quickly centrifuge them, place them in a heated muffle furnace, and increase the temperature to a level high enough for calcination. After grinding into a fine powder, the NMs are stored for later use. Comprehensive procedure for the green synthesis of iron ferrite nanoparticles using Mango, Neem, and Moringa leaves extracts.

Figure 3.1: Synthesis of Green Ferrite at constant temperature

Figure 3.2: Separation of Nano Ferrite particles by using Centrifuge.

Figure 3.3: For Pre heating and calcination of sample at 800 °C

3.2. MATERIALS USED

Fresh Mango/Neem/Moringa leaves Powder

- Iron(II) chloride tetrahydrate ($FeCl_2 \cdot 4H_2O$)
- Iron(III) chloride hexahydrate ($FeCl_3 \cdot 6H_2O$)
- Deionized water
- Sodium hydroxide (NaOH) solution (1 M)
- Beakers, burette, magnetic stirrer, oil bath
- Centrifuge, pH paper or meter
- Freezer dryer or oven

3.3. PROCEDURE

Preparation of Leaf Extracts

- Wash 10–20 g of fresh Mango or Neem leaves thoroughly with distilled water to remove surface contaminants.
- Boil leaves in 100 mL deionized water at 80 °C for 20 minutes.
- Cool the extract to room temperature and filter through Whatman No.1 filter paper to remove solid debris, collecting the clear extract for use.

Preparation of Iron Salt Solution

- Dissolve 0.40 g $FeCl_2 \cdot 4H_2O$ and 1.10 g $FeCl_3 \cdot 6H_2O$ (1:2 molar ratio) in 100 mL deionized water.
- Place the beaker with iron solution on a magnetic stirrer and heat the mixture to 80 °C for 10 minutes to ensure homogeneity. [10]

Synthesis Reaction

- Add 5 mL of the prepared mango, Neem or Eucalyptus leaf extract drop wise into the hot iron salt solution under continuous stirring.
- While stirring, add 20 mL of 1 M NaOH solution slowly (drop-by-drop) using a burette, over a period of 30 minutes. This step should be maintained at 80 °C for the full duration.
- The solution should show an instantaneous colour change (from pale yellow/orange to black), indicating the formation of iron ferrite nanoparticles.
- Continue stirring for an additional 30 minutes after full addition of NaOH.

Cooling and Separation

- Allow the reaction mixture to cool to room temperature.
- Separate the black Nanoparticles by magnetic decantation or centrifugation at 5000 rpm for 10 minutes.

Washing and Purification

- Wash the collected nanoparticles with 15 mL deionized water; centrifuge again at 5000 rpm for 10 minutes.
- Discard the supernatant and repeat the wash with 10 mL deionized water once more.
- If needed, wash further with ethanol to remove any residual organic compounds.

Drying

- Collect the washed nanoparticles and dry overnight on hot Oven.

Calcination

- For optimal ferrite crystal growth and enhanced magnetic properties, calcination is typically carried out at around 800 °C for 5–6 hours.

Figure 3.4: Process of Green synthesis of Nano ferrites from Different leaves

CHAPTER 4
CHARACTERIZATION

4. CHARACTERIZATION

The following are the different methods used for characterization of Nano particles. Some of the methods are given below

4.1. X-RAY DIFFRACTION METHOD

X-ray diffraction is a versatile, non-destructive analytical method for identification and quantitative determination of various crystalline forms, known as 'phases' of compound present in powder and solid samples. Diffraction occurs as waves interact with a regular structure whose repeat distance is about the same as the wavelength. The phenomenon is common in the natural world, and occurs across a broad range of scales. For example, light can be diffracted by a grating having scribed lines spaced on the order of a few thousand angstroms, about the wavelength of light. It happens that X-rays have wavelengths on the order of a few angstroms, the same as typical inter-atomic distances in crystalline solids. That means X-rays can be diffracted from minerals which, by definition, are crystalline and have regularly repeating atomic structures. When certain geometric requirements are met, X-rays scattered from a crystalline solid can constructively interfere, producing a diffracted beam. In 1912, W. L. Bragg recognized a predictable relationship among several factors.

The distance between similar atomic planes in a mineral (inter atomic spacing) which we call the d-spacing and measure in angstroms.

The angle of diffraction which we call the theta angle and measure in degrees. For practical reasons the Diffractometer measures an angle twice that of the theta angle. Not surprisingly, we call the measured angle '2-theta'.

The wavelength of the incident X-radiation, symbolized by the Greek letter lambda and, in our case, equal to 1.54 angstroms.

The unit cell and lattices which are distributed in a regular three-dimensional space forms the base for diffraction pattern to occur. These lattices form a series of parallel planes with its own specific d-spacing and with different orientations exist. The reflection of incident monochromatic X-ray from successive planes of crystal lattices when the difference between the planes is of a complete n number of wavelengths leads to a famous Bragg's law:

$$\mathbf{n\lambda = 2d\sin\theta}$$

λ - Wavelength of X-ray in armstroms d - Interplanar spacing

θ - Diffraction angle in degrees

n - Integer 1, 2, 3…. (Usually equal to 1)

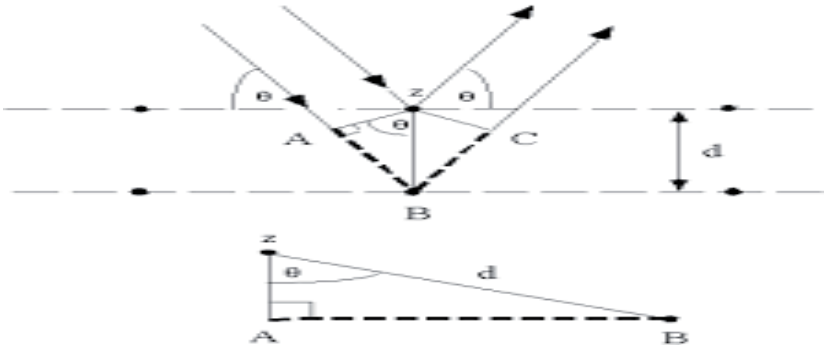

Figure 4.1: Bragg's diffraction

Plotting the angular positions and intensities of the resultant diffracted peaks of radiation produces a pattern, which is characteristic of the sample. The fingerprint characterization of crystalline materials and the determination of their structure are the two fields where XRD has been mostly used. Unique characteristic X-ray diffraction pattern of each crystalline solid gives the designation of "fingerprint technique" to XRD for its identification. XRD may be used to determine its structure, i.e. how the atoms pack together in the crystalline state and what the interatomic distance and angle are etc. The crystallite size can be found out by using the Scherer's formula,

$$P = \frac{0.9\lambda}{\beta\cos\theta}$$

Where

P - Crystallite size; λ - Wavelength

β - Full maxima half width; θ- Diffraction angle

Figure 4.2: Diffractometer (Model: DY-1656)

From these points it can be concluded that X-ray diffraction has become a very important and powerful tool for the structural characterization in solid state physics and materials science.

4.2. SCANNING ELECTRON MICROSCOPE (SEM)

The scanning electron microscope (SEM) uses a focused beam of high-energy electrons to generate a variety of signals at the surface of solid specimens. The signals that derive from electron sample interactions reveal information about the sample including external morphology (texture), chemical composition, and crystalline structure and orientation of materials making up the sample. In most applications, data are collected over a selected area of the surface of the sample, and a 2-dimensional image is generated that displays spatial variations in these properties. Areas ranging from approximately 1cm to 5microns in width can be imaged in a scanning mode using conventional SEM techniques (magnification ranging from 20X to approximately 30,000X, spatial resolution of 50 to 100 nm). The SEM is also capable of performing analyses of selected point locations on the sample; this approach is especially useful in qualitatively or semi-quantitatively determining chemical compositions (using EDS), crystalline structure, and crystal orientations (using EBSD). The design and function of the SEM is very similar to the EPMA, and considerable overlap in capabilities exists between the two instruments.

Figure 4.3: SEM (JEOL-JSM 5800)

Fundamental Principles of Scanning Electron Microscopy (SEM)

Accelerated electrons in an SEM carry significant amounts of kinetic energy, and this energy is dissipated as a variety of signals produced by electron-sample interactions when the incident electrons are decelerated in the solid sample. These signals include secondary electrons (that produce SEM images), back scattered electrons (BSE), diffracted back scattered electrons (EBSD that are used to determine crystal structures and orientations of minerals), photons (characteristic X-rays that are used for elemental analysis and continuum X-rays), visible light (cathode luminescence--CL), and heat. Secondary electrons and

backscattered electrons are commonly used for imaging samples: secondary electrons are most valuable for showing morphology and topography on samples and backscattered electrons are most valuable for illustrating contrasts in composition in multiphase samples (i.e. for rapid phase discrimination).

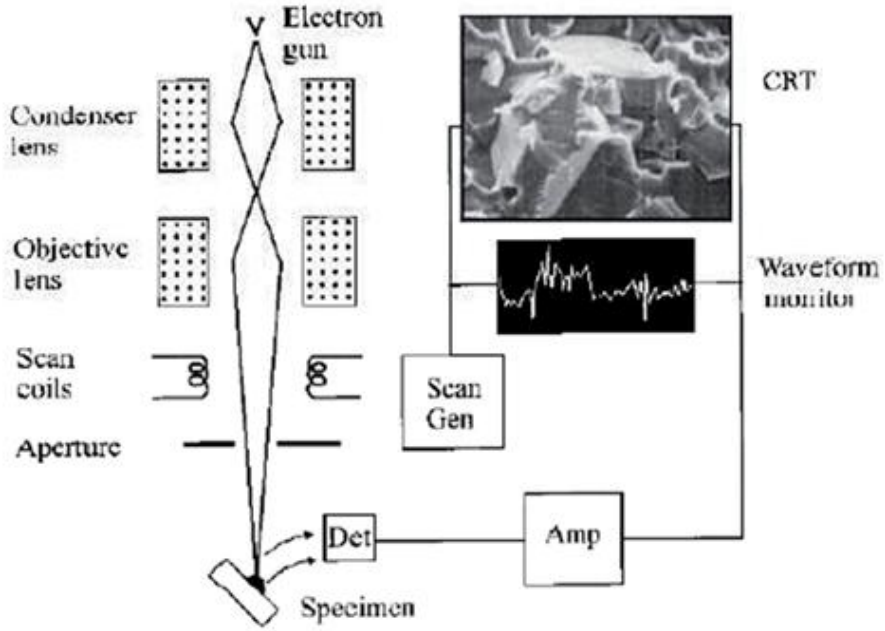

Figure 4.4: Schematic Diagram of SEM

X-ray generation is produced by inelastic collisions of the incident electrons with electrons in discrete orbitals (shells) of atoms in the sample. As the excited electrons return to lower energy states, they yield X-rays that are of a fixed wavelength (that is related to the difference in energy levels of electrons in different shells for a given element). Thus, characteristic X-rays are produced for each element in a mineral that is "excited" by the electron beam. SEM analysis is considered to be "non-destructive"; that is, x-rays generated by electron interactions do not lead to volume loss of the sample, so it is possible to analyze the same materials repeatedly.

The SEM is routinely used to generate high-resolution images of shapes of objects (SEI) and to show spatial variations in chemical compositions: 1) acquiring elemental maps or spot chemical analyses using EDS, 2) discrimination of phases based on mean atomic number (commonly related to relative density) using BSE, and 3) compositional maps based on differences in trace element "activators" (typically transition metal and Rare Earth elements) using CL. The SEM is also widely used to identify phases based on qualitative chemical analysis and/or crystalline structure. Precise measurement of very small features and objects down to 50nm in size is also accomplished using the SEM.

4.3. TRANSMISSION ELECTRON MICROSCOPE (TEM)

Electron Microscopes are scientific instruments that use a beam of highly energetic electrons to examine objects on a very fine scale. This examination can yield the information like topography, morphology, composition as well as crystallographic information's. Working principle is exactly as their optical counter parts except that they use a focused beam of electrons instead of light to "image" the specimen and gain information as to its structure and composition.

The main use of this technique is to examine the specimen structure, composition or properties in submicroscopic details so that this microscopy technique is significantly involved in numerous fields. In TEM there is no change in the refractive index of the medium when the illumination beam is deflected, the vacuum in the lens is the same as the vacuum in the column. Deflection is in this case only due to the electromagnetic properties of the lens which are defined by electromagnetic plates that are only able to influence the path direction of the electrons, since all of the electrons carry a negative charge. Those electrons that pass through the sample go on to form the image while those that are stopped or deflected by dense atoms in the specimen are subtracted from the image.

In this way a black and white image is formed. Remaining other electrons which passes close to heavy atoms and get only slightly deflected make their way down the column and contribute to the image. There are three main reasons why the microscope column must be operated under very high vacuum. The first of these is to avoid collisions between electrons of the beam and stray molecules. Such collisions can result in a spreading or diffusing of the beam or more seriously can result in volatization event if the molecule is organic in nature. Such volatization can severely contaminate the microscope column especially in finely machined regions such as apertures and pole pieces that will serve to degrade the image.

4.4. UV-VISIBLE SPECTROSCOPY

The wavelength of UV is shorter than the visible light. It ranges from 100 to 400 nm. In a standard UV-Vis spectrophotometer, a beam of light is split; one half of the beam (the sample beam) is directed through a transparent cell containing a solution of the compound being analysed, and one half (the reference beam) is directed through an identical cell that does not contain the compound but contains the solvent. The instrument is designed so that it can make a comparison of the intensities of the two beams as it scans over the desired region of the wavelengths. If the compound absorbs light at a particular wavelength, the intensity of the sample beam (IS*)* will be less than that of the reference beam. Absorption of radiation by a sample is measured at various wavelengths and plotted by a recorder to give the spectrum which is a plot of the wavelength of the entire region versus the absorption (A)

of light at each wavelength**.** And the band gap of the sample can be obtained by plotting the graph between (ah vs hv) and extrapolating it along x-axis**.** Ultraviolet and visible spectrometry is almost entirely used for quantitative analysis; that is, the estimation of the amount of a compound known to be present in the sample. The sample is usually examined in solution.

Figure 4.5: UV- Vis Spectrophotometer with COD

4.5. FOURIER TRANSFORM INFRARED SPECTROMETER (FTIR)

An FTIR spectrometer is an analytical instrument that measures the infrared absorption spectrum of a sampleallowing identification and characterization of molecular structures based on their vi brational transitions.

FTIR (Fourier Transform Infrared) spectroscopy is based on the fact that molecules absorb infrar ed radiation at specific frequencies corresponding to their vibrational and rotational motions. Unl ike dispersive IR spectroscopy, which scans one wavelength at a time, FTIR collects all wavelen gths simultaneously and uses a mathematical Fourier Transform to convert the recorded interfero gram into a conventional spectrum of absorbance or transmittance versus wavenumber (cm^{-1}).

The core components include:

Interferometer: Usually, a Michelson interferometer that splits and recombines the IR beam to c reate an interference pattern (interferogram).

- **IR Source**: Emits broadband infrared radiation.
- **Sample Holder**: Can accommodate gas cells, liquid cells, or thin solid films.
- **Detector**: Measures the intensity of the interfered IR light after the sample interaction.
- **Computer and Software**: Performs Fourier Transform to convert the interferogram into a usable spectrum.

Process

- Infrared light passes through the interferometer, generating an interferogram that encodes all the frequency components simultaneously.

- The beam passes through the sample, and specific frequencies are absorbed according to t he chemical bonds present.
- The detector records intensity variations as a function of path difference.
- A Fourier Transform algorithm converts the interferogram into an absorption or transmitt ance spectrum as a function of wavenumber.
- Peaks in the spectrum correspond to specific vibrational transitions of functional groups i n the molecule.

Applications

FTIR is widely used in chemistry, materials science, and industry for:

- Identification of organic and inorganic compounds based on characteristic absorption ban ds.
- Quality control and process monitoring in pharmaceuticals, polymers, and chemicals.
- Study of molecular interactions such as hydrogen bonding, conformational changes, and polymer crystallinity.
- Surface and thin film analysis using ATR (Attenuated Total Reflectance) accessories.
- Environmental monitoring, e.g., detecting greenhouse gases and pollutants.

Advantages of FTIR

- Fast data acquisition due to simultaneous collection of all wavelengths.
- High sensitivity and resolution with appropriate interferometer settings.
- Minimal sample preparation for ATR or diffuse reflectance methods.
- Quantitative analysis potential because absorption intensity is proportional to concentrati on.
- Versatility, being applicable to solids, liquids, and gases.

Figure 4.6: Fourier Transform Infrared Spectrometer (FTIR)

CHAPTER 5

RESULTS AND DISCUSSION

Photo catalytic degradation of organic pollutants is a promising technology because it can mineralize toxic contaminants into harmless end products. Dye effluents from textile industries pose a serious environmental problem due to their intense and persistent color. Spinel Nano ferrites are well-known photo catalysts and have been widely explored for the degradation of methylene blue and other organic dyes under light irradiation. During the Photocatalytic experiment, the degradation of methylene blue generally increases as a function of irradiation time when Nano ferrite is used as the catalyst. In many studies, the decomposition ratio for methylene blue reaches about 80–90% within 2–3 hours under optimized conditions such as suitable pH, catalyst loading, and dye concentration, confirming the good activity of Nano ferrites toward dye degradation. Hence, Nano ferrites can be regarded as effective catalysts for degrading different dyes, and the photo catalytic reaction rate depends strongly on parameters like irradiation time, catalyst dose, and solution pH. Nano ferrite nanoparticles are commonly synthesized by the Co-precipitation route because it provides good control over particle size, homogeneity, and phase purity. The as-prepared nano ferrites are typically characterized by X-ray Diffraction (XRD) and Fourier Transform Infrared Spectrometer (FTIR) to confirm their nanoscale morphology, particle size distribution, and degree of agglomeration before using them in photo catalytic dye degradation studies.

5.1. X-RAY DIFFRACTION (XRD) RESULTS

5.1.1. For Sample 1

First Sanple 1, for Nano ferrite was synthesized using Moringa leaf powder by the already-mentioned green synthesis process. The synthesized sample was analyzed by X-ray Diffraction (XRD) at Central Research Facility, Maulana Azad National Institute of Technology (MANIT), Bhopal. The XRD pattern confirmed the presence of Nano ferrites in the sample, specifically Copper Ferrite ($CuFe_2O_4$), Magnesium Ferrite ($MgFe_2O_4$), and Manganese Ferrite ($MnFe_2O_4$). The phases were identified and characterized by matching the diffraction peaks with the standard Joint Committee on Powder Diffraction Standards (JCPDS) cards.

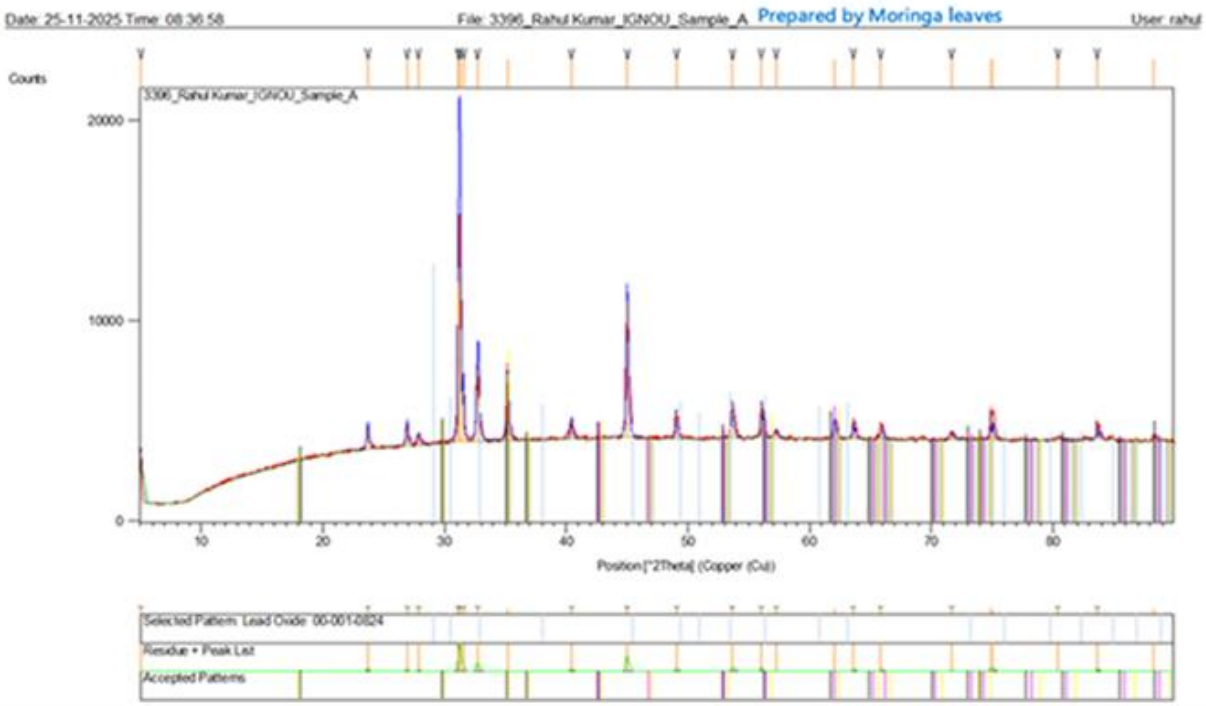

Figure 5.1: XRD Analysis of Sample 1

The JCPDS card references for these ferrite phases are as follows

- **COPPER FERRITE ($CuFe_2O_4$)**

Parameter	Details
Reference code	01-077-0010
Compound name	Copper Iron Oxide
ICSD name	Copper Iron Oxide
Empirical formula	$CuFe_2O_4$
Chemical formula	$CuFe_2O_4$

- **MAGNESIUM FERRITE ($MgFe_2O_4$)**

Parameter	Details
Reference code	96-900-3600
Mineral name	Magnesioferrite
Compound name	Magnesioferrite
Common name	Magnesioferrite
Chemical formula	$Fe_{16.00}Mg_{8.00}O_{32.00}$

- **MANGANESE FERRITE ($MnFe_2O_4$)**

Parameter	Details
Reference code	00-010-0319
Mineral name	Jacob site (synthetic)
Compound name	Manganese Iron Oxide
PDF index name	Manganese Iron Oxide
Empirical formula	Fe_2MnO_4
Chemical formula	$MnFe_2O_4$

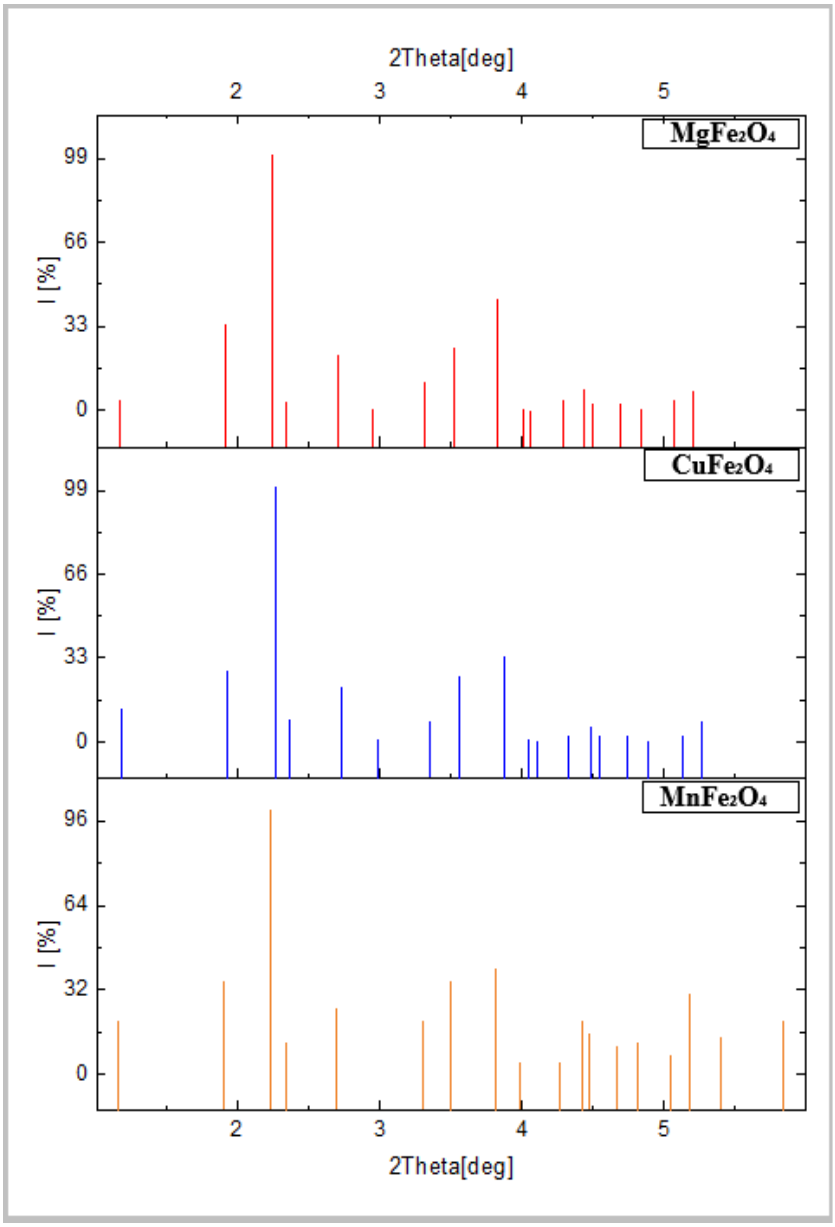

Figure 5.2: XRD graph for peaks Intensity & 2 Theta [deg]

Crystallographic Parameters are same for all Ferrites.

Parameter	Details
Crystal system	Cubic
Space group	Fd-3m
Space group number	227

5.1.2. For Sample 2

Then, sample 2 synthesized using Mango leaf powder by the already-mentioned green synthesis process and also the synthesized sample was analyzed by X-ray Diffraction (XRD) at Central Research Facility, Maulana Azad National Institute of Technology (MANIT), Bhopal. The XRD pattern confirmed the presence of Nano ferrites in the sample with space group Fd3m. specifically Nickel ferrite ($NiFe_2O_4$), Magnesium ferrite ($MgFe_2O_4$), and Zinc ferrite ($ZnFe_2O_4$). The phases were identified and characterized by matching the diffraction peaks with the standard Joint Committee on Powder Diffraction Standards (JCPDS) cards.

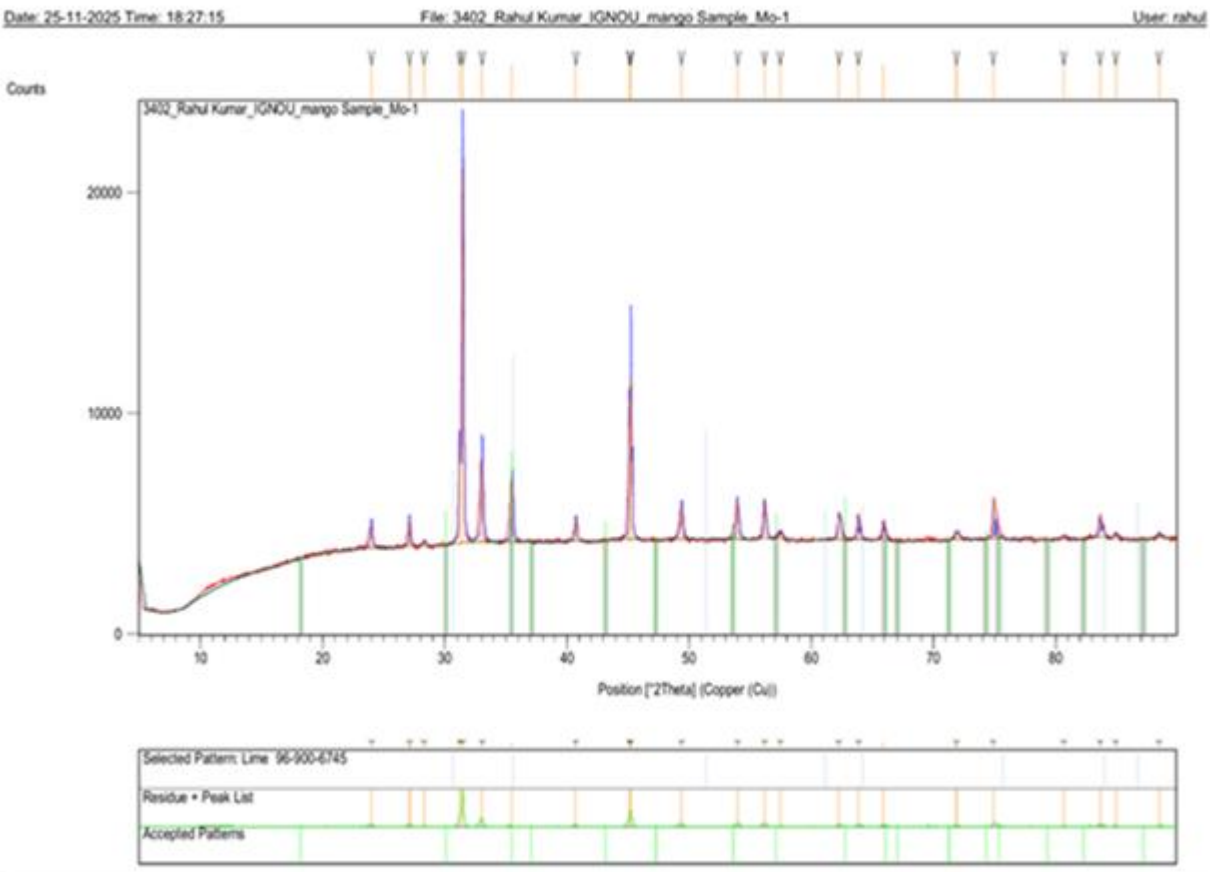

Figure 5.3: XRD Analysis of Sample 2

The JCPDS card references for these ferrite phases are as follows:

- **MAGNESIUM FERRITE ($MgFe_2O_4$)**

Parameter	Details
Reference code	96-900-3783
Mineral name	Magnesioferrite
Compound name	Magnesioferrite
Common name	Magnesioferrite
Chemical formula	$Mg_{8.00}Fe_{16.00}O_{32.00}$

- **NICKLE FERRITE ($NiFe_2O_4$)**

Parameter	Details
Reference code	00-003-0875
Compound name	Nickel Iron Oxide
PDF index name	Nickel Iron Oxide
Empirical formula	Fe_2NiO_4
Chemical formula	$NiFe_2O_4$

- **ZINC FERRITE ($ZnFe_2O_4$)**

Parameter	Details
Reference code	00-001-1109
Compound name	Zinc Iron Oxide
PDF index name	Zinc Iron Oxide
Empirical formula	Fe_2O_4Zn
Chemical formula	$ZnFe_2O_4$

Crystallographic Parameters are same for all Ferrites.

Parameter	Details
Crystal system	Cubic
Space group	Fd-3m
Space group number	227

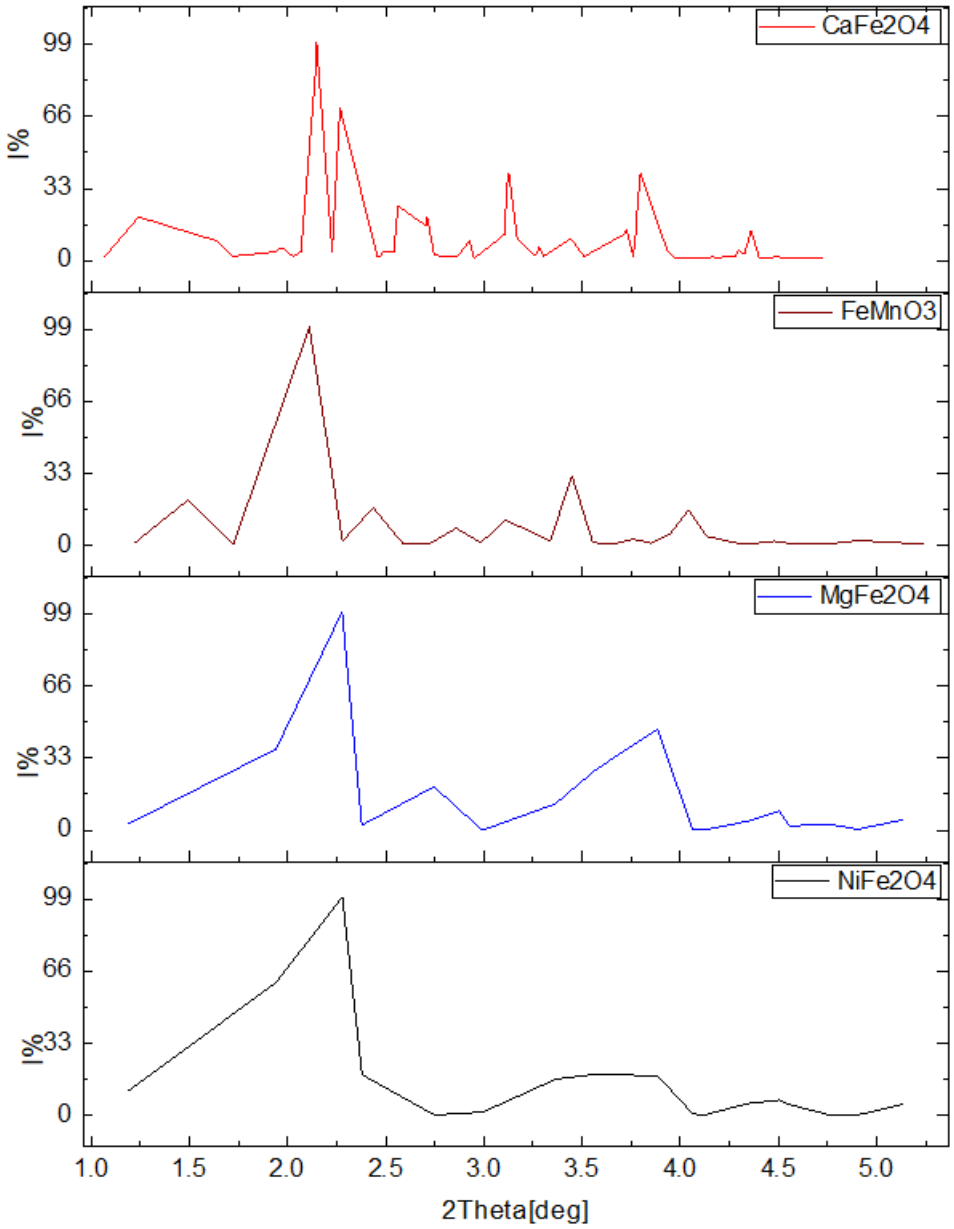

Figure 5.4: XRD graph for peaks Intensity & 2 Theta [deg]

5.1.3. For Sample 3

Last sample for, Nano ferrite was synthesized using Neem leaf powder by the already-mentioned green synthesis process. The synthesized sample was also analyzed by X-ray Diffraction (XRD) at Central Research Facility, Maulana Azad National Institute of Technology (MANIT), Bhopal. The XRD pattern confirmed the presence of Nano ferrites in the sample, specifically Magnesium ferrite ($MgFe_2O_4$), and Zinc ferrite ($ZnCr_2O_4$) and $ZnCo_2O_4$. The phases were identified and characterized by matching the diffraction peaks with the standard Joint Committee on Powder Diffraction Standards (JCPDS) cards.

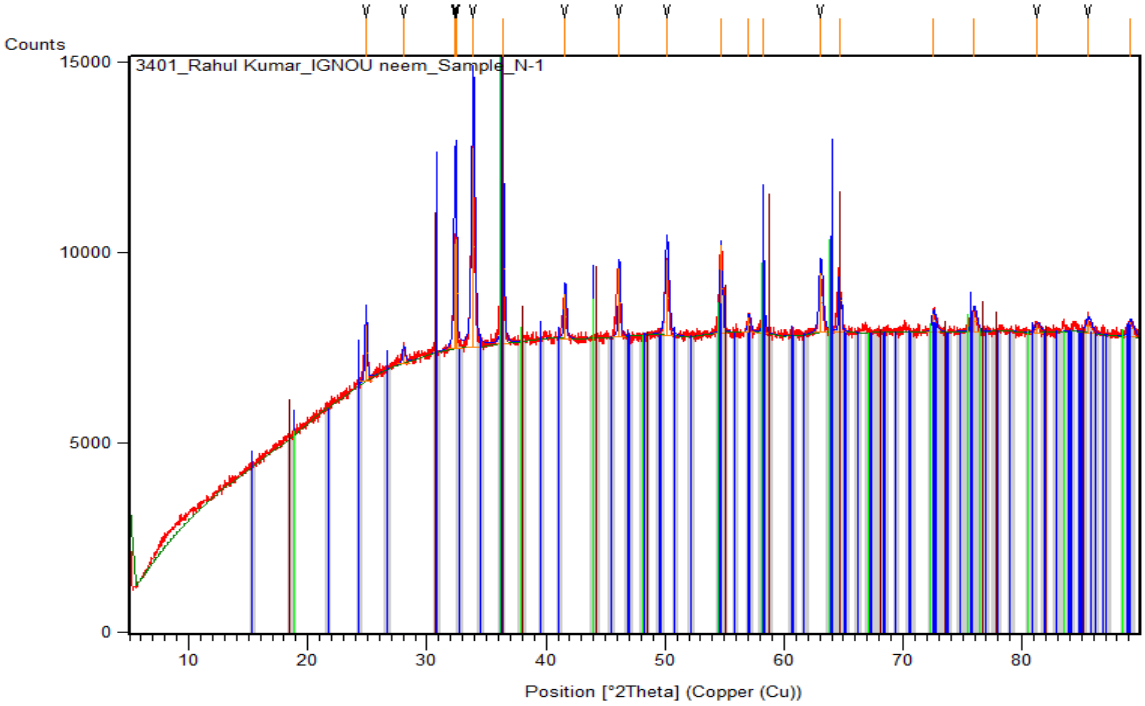

Figure 5.5: XRD Analysis of Sample 3

The JCPDS card references for these ferrite phases are as follows:

- **MAGNESIUM FERRITE ($MgFe_2O_4$)**

Parameter	Details
Reference code	96-901-0294
Compound name	9010293
Common name	9010293
Chemical formula	$Mg_{4.00}Fe_{8.00}O_{16.00}$

- **ZINC FERRITE ($ZnCr_2O_4$)**

Parameter	Details
Reference code	01-073-1962
Compound name	Zinc Chromium Oxide
ICSD name	Zinc Chromium Oxide
Empirical formula	Cr_2O_4Zn
Chemical formula	$ZnCr_2O_4$

- **ZINC FERRITE ($ZnCo_2O_4$)**

Parameter	Details
Reference code	00-023-1390
Compound name	Zinc Cobalt Oxide
PDF index name	Zinc Cobalt Oxide
Empirical formula	Co_2O_4Zn
Chemical formula	$ZnCo_2O_4$

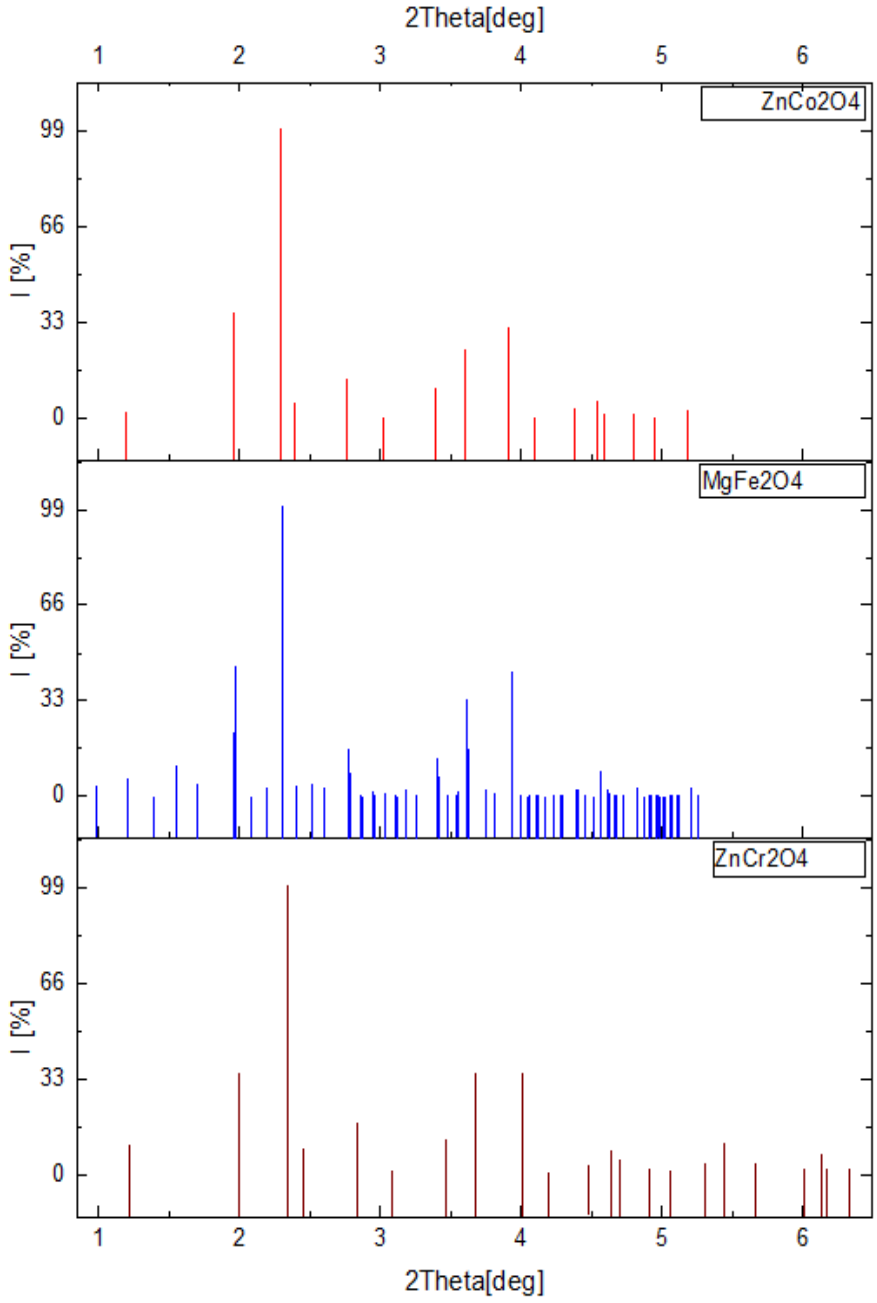

Figure 5.6: XRD graph for peaks Intensity & 2 Theta [deg]

XRD analysis of all three samples confirms the presence of nanoferrite particles, primarily composed of Copper Ferrite ($CuFe_2O_4$), Magnesium Ferrite ($MgFe_2O_4$), Manganese Ferrite ($MnFe_2O_4$), and Zinc Ferrite ($ZnCr_2O_4$) in the MAB_2O_4 spinel structure. Therefore, these samples can be further utilized for dye degradation experiments.

5.2. FTIR ANALYSIS RESULT

All synthesized sample was also analyzed by Fourier Transform Infrared Spectrometer (FTIR) at Central Research Facility, Maulana Azad National Institute of Technology (MANIT), Bhopal. The FTIR pattern confirmed the presence of Nano ferrites in the all sample.

5.2.1 for sample 1

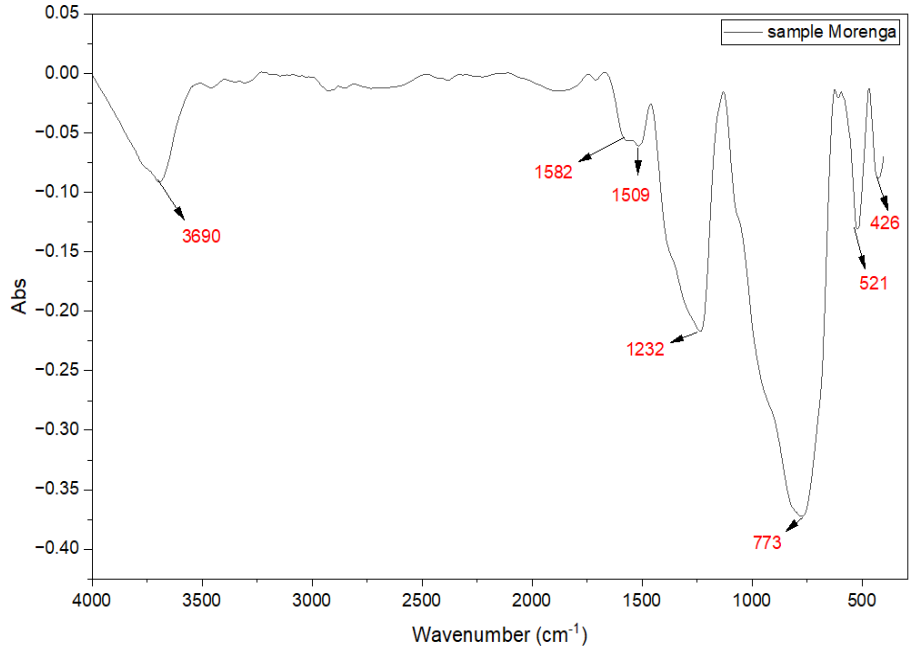

Figure 5.7: FTIR graph for ferrite sample 1 which is synthesis by Moringa powder

The spectrum supports the presence of a ferrite phase in sample 1 (Moringa sample). The strong bands at 521 and 426 cm^{-1} correspond to metal–oxygen (M–O) stretching vibrations in tetrahedral and octahedral sites of a spinel ferrite lattice.

Ferrite Bands (400–800 cm^{-1})

- Spinel ferrites characteristically show two main absorption bands between about 400 and 800 cm^{-1}, assigned to tetrahedral (A-site) and octahedral (B-site) M–O stretching vibrations.[21]
- Fe_3O_4 and related ferrites typically show strong Fe–O bands around 550–600 cm^{-1} (A-site) and 400–450 cm^{-1} (B-site), with some compositional shifts.[22]
- In this spectrum, the intense peaks at ~521 and ~426 cm^{-1} fall squarely in this ferrite window and match literature values for Fe–O vibrations in spinel ferrites, indicating formation of a ferrite lattice rather than only organic moringa.

Other functional groups

Other functional groups also identified in the sample are derived from the Moringa leaf extract.

- The broad feature near 3690 cm^{-1} is consistent with O–H stretching of adsorbed water and phenolic hydroxyl groups from Moringa leaf constituents, similar to reported O–H bands around 3200–3400 cm^{-1} in Moringa extracts.[23]
- Peaks at 1582 and 1509 cm^{-1} can be assigned to C=C or C=O related vibrations of aromatic/phenolic compounds, and the band at 1232 cm^{-1} to C–O stretching, all typical for moringa phytochemicals.[24]
- The band around 773 cm^{-1} may reflect C–H out-of-plane bending or residual organics; its presence alongside strong M–O bands suggests ferrite nanoparticles still coated or capped with organic species from the moringa precursor.

5.2.2. For Sample 2

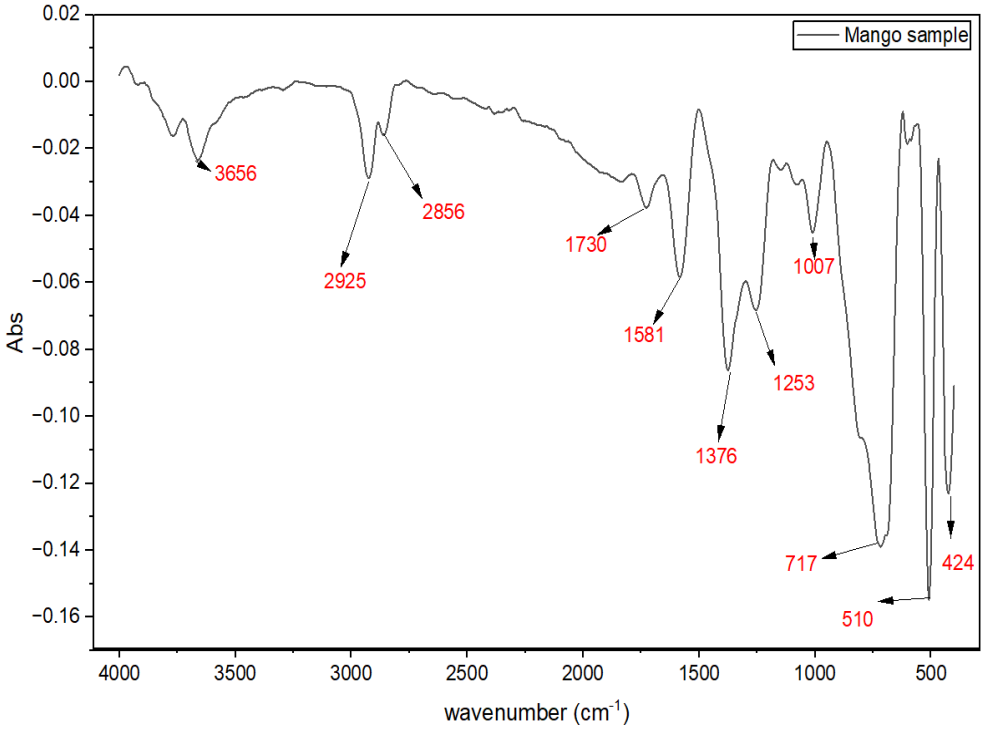

Figure 5.8: FTIR graph for Ferrite sample 2 which is synthesis by Mango powder

The ferrite phase is present in this mango-based sample, as indicated by the strong bands at about 510 and 424 cm^{-1} which correspond to metal–oxygen vibrations in a spinel ferrite lattice.

Ferrite Bands

- Spinel ferrites typically show two main FTIR bands between about 400 and 800 cm^{-1}, assigned to tetrahedral (A-site) and octahedral (B-site) metal–oxygen (M–O) stretching vibrations.

- Reported Fe_3O_4 and mixed ferrites often display intense bands around 500–600 cm^{-1} (tetrahedral M–O) and 400–450 cm^{-1} (octahedral M–O).
- This spectrum shows two clear, sharp peaks near 510 and 424 cm^{-1}, matching these ferrite M–O ranges and confirming formation of a spinel-type ferrite phase rather than only organic mango components.

Organic and surface functional groups

- The broad band at 3656 cm^{-1} corresponds to O–H stretching of adsorbed water and hydroxyl/phenolic groups from mango leaf phytochemicals, similar to O–H bands commonly reported for plant extracts.
- Peaks near 2925 and 2856 cm^{-1} arise from C–H stretching of aliphatic chains, while the 1730 cm^{-1} band indicates C=O stretching of carbonyl or ester groups from biomolecules.
- Bands at 1581, 1376, 1253 and 1007 cm^{-1} can be attributed to C=C, C–H bending and C–O stretching modes of residual organic species, showing that plant-derived ligands still cap or coat the ferrite nanoparticles.
- The coexistence of distinct ferrite M–O bands at 510 and 424 cm^{-1} with characteristic O–H, C–H, C=O and C–O bands from mango phytochemicals indicates successful formation of spinel ferrite nanoparticles stabilized by organic moieties.

5.2.3. For Sample 3

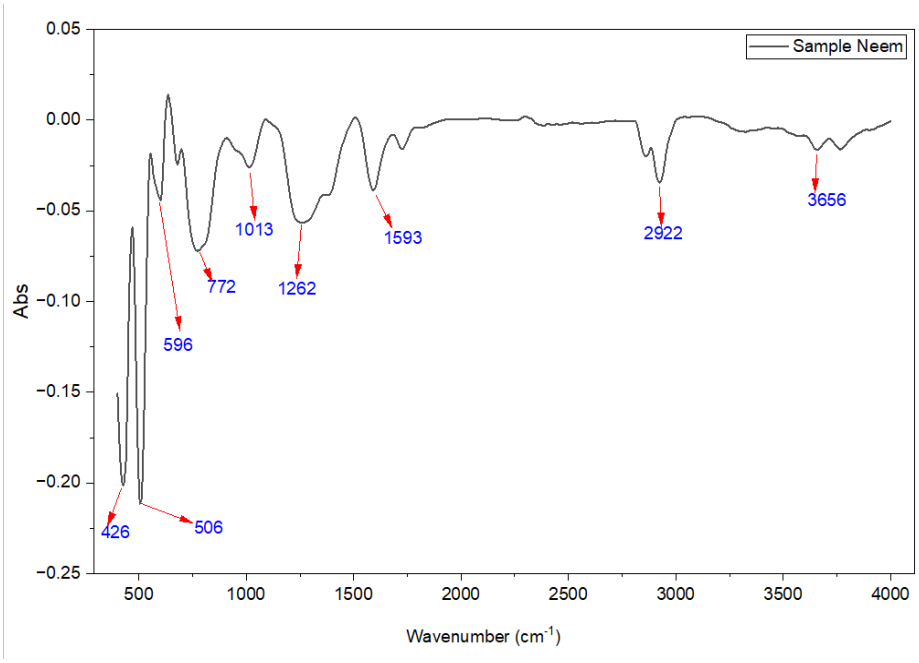

Figure 5.9: FTIR graph for Ferrite sample 3 which is synthesis by Neem powder

This Neem-based sample also shows the ferrite phase, mainly evidenced by the strong bands at about 596, 506 and 426 cm^{-1} that correspond to metal–oxygen vibrations of a spinel ferrite lattice

Ferrite M–O bands (400–800 cm^{-1})

- Fe_3O_4 and other spinel ferrites commonly reports intense bands between about 550–600 cm^{-1} and 400–450 cm^{-1} for these M–O vibrations.
- The clear peaks at ~596, ~506 and ~426 cm^{-1} in your spectrum fall within this ferrite window and are consistent with Fe–O (and other metal–O) stretching in spinel ferrites, indicating formation of a ferrite phase rather than only Neem organics.

Other functional groups

Other functional groups also identified in the sample are derived from the Neem leaf extract.

- The broad band at 3656 cm^{-1} corresponds to O–H stretching from adsorbed water and hydroxyl/phenolic groups, typical for Neem leaf extracts and plant phytochemicals.
- The 2922 cm^{-1} band arises from C–H stretching of aliphatic chains; bands at 1593, 1262, 1013 and 772 cm^{-1} can be assigned to C=C, C–N/C–O stretching and C–H bending modes of residual organic compounds from Neem.
- The simultaneous presence of distinct low-wavenumber M–O bands (596, 506, 426 cm^{-1}) with higher-wavenumber O–H, C–H, C=C and C–O bands shows that spinel ferrite nanoparticles have formed and are capped or stabilized by Neem-derived organic species.

5.3. PHOTO CATALYTIC STUDY OF FERRITE PARTICLES

A major chunk of pollutants in contaminated water is from synthetic textile dyes and industrial dyes. Metal Ferrite (Mg, MN Ni Zn… ferrites) Nanoparticles have been used to study the photo catalytic degradation of various dyes like Methylene Blue. [25]

Preparation of Dye Solutions

Stock solution of methylene blue was prepared by dissolving 0.05 ml of dye in 100 mL of distilled water.

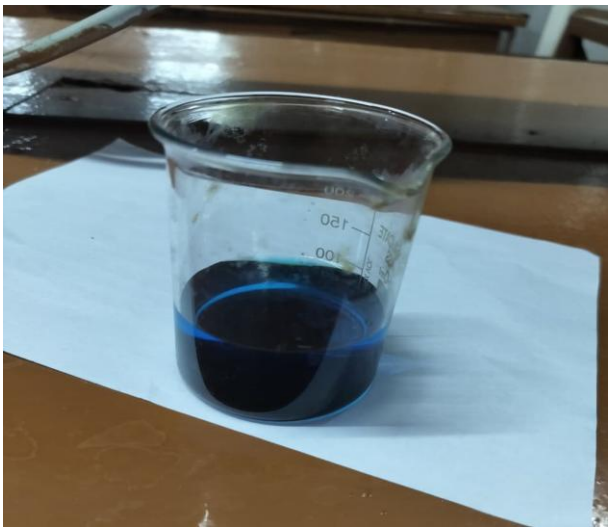

Figure 5.10: Solution of Methylene Blue in distilled water

For Sample 1

From the prepared dye stock solution, add 0.2 g of the ferrite sample synthesized using Moringa leaf extract.

5.4. PHOTO CATALYTIC DEGRADATION OF METHYLENE BLUE UNDER SUN LIGHT

To evaluate the effectiveness of Ferrite particles as photo catalyst, MB solution was used as a model compound. The mixture of MB solution with Ferrite particles was exposed to Sun (UV) light. The color of MB slowly faded when exposed to Sun (UV) light for 0 hours, 2 hours, 4 hours, 6 hours.

Figure 5.11: Mixture of MB solution with Ferrite particles expose to sunlight light.

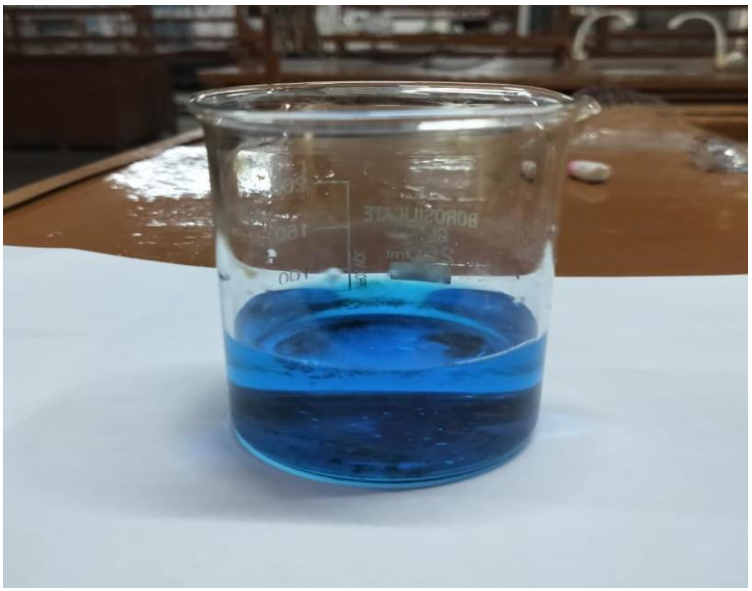

Figure 5.12: solution after 2 hours

Figure 5.13: Degradation of MB under sunlight after 6 hours.

For Sample 2

From the prepared dye stock solution, add 0.2 g of the ferrite sample synthesized using Mango leaf extract.

Figure 5.14: Mixture of MB solution with Ferrite particles expose to sunlight light

Figure 5.15: solution after 3 hours

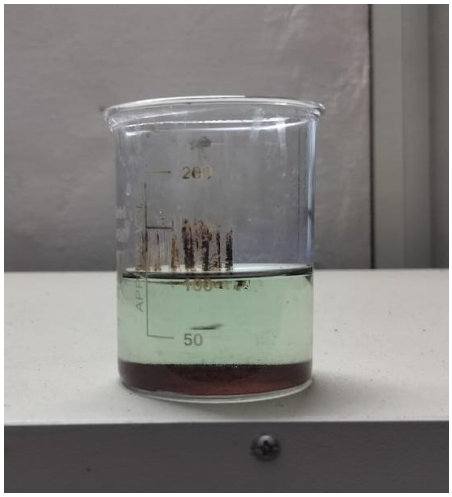

Figure 5.16: Degradation of MB under sunlight after 6 hours

For Sample 3

From the prepared dye stock solution, add 0.2 g of the ferrite sample synthesized using Neem leaf extract.

Figure 5.17: Mixture of MB solution with Ferrite particles expose to sunlight light.

Figure 5.18: solution after 3 hours

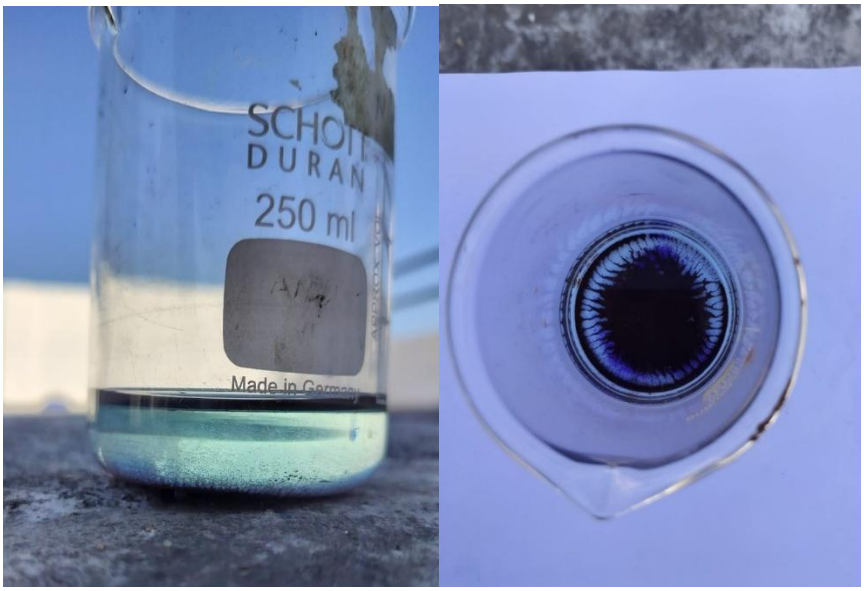

Figure 5.19: Degradation of MB under sunlight after 6 hours.

The degradation of MB solution by Ferrite Nano particles could be explained by mechanism below-

When MFe_2O_4 particles were illuminated by UV light with energy greater than the band gap energy, the conduction-band electrons (e−CB) and valence-band holes (h+VB) were generated on the surfaces of MFe_2O_4 particles Holes could react with water adhering to the surfaces of MFe_2O_4 particles to form highly reactive hydroxyl radicals (•OH). Meanwhile, oxygen acted as an electron acceptor by forming a super oxide radical anion (O•−2) MB was believed to be destroyed through direct oxidation by the •OH radicals and O•−2 radicals as shown

$$MFe_2O_4 + hv\ (UV)^{-} \longrightarrow e_{CB}^{-} + h_{VB}^{+}$$

$$h_{VB}^{+} + H_2O^{-} \longrightarrow H^{+} + {}^{\bullet}OH$$

$$eCB^{-} + O2^{-} \longrightarrow O2^{\bullet -}$$

$$O_2^{\bullet -} + \cdot OH + dye^{-} \longrightarrow \text{degraded product}$$

Photo catalytic testing

The optical and photo catalytic properties of the samples were investigated by measuring the UV and visible light absorption at room temperature using a Spectrophotometer. Since the photo catalytic degradation of methylene blue occurs predominantly on the surface of photo catalyst, studies on the adsorption of the dyes from aqueous solution onto MFe_2O_4 particles are relevant and important. The equilibrium concentration of the methylene blue in contact with the catalyst, instead of that of the feed dye solution, represents the true methylene blue concentration in

solution at the start of irradiation. For solar light exposure, experiments were performed on a bright sunny day in an open space between 09:00 to 16:00 hours. The MB degradation during the course of reaction (1hour, 2hours, 3hours, 4hours, 6hours) was followed by recording its optical absorbance maxima at 653nm, while establishing a baseline data set with MB solutions exposed directly to various light conditions without addition of any MFe_2O_4 [2].

Photo catalytic Degradation of MB

The dye is used because of its absorption peaks in visible range. Figure shows that absorption peak is achieved at 653nm. Some intermediates would be formed during methylene degradation, and the major absorption band of methylene blue and its degradation intermediates was around 665 nm.

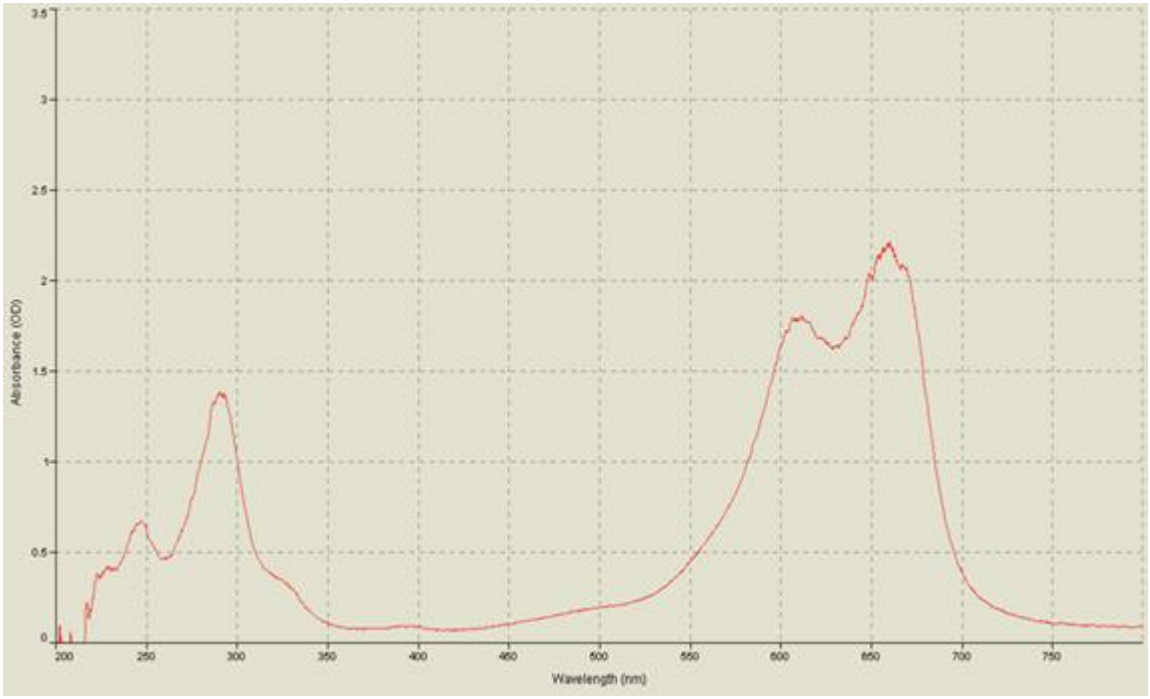

Figure 5.20: Absorption graph of Methylene Blue

In order to investigate the photo catalytic activities of Ferrite MFe_2O_4 the mineralization of methylene blue was evaluated according to the absorption change in this work. The decomposition of methylene blue was monitored by measuring the absorbance of the solution using the UV– Vis spectrophotometer at (653nm) in liquid cuvette configuration with de-ionized water as reference.

Figure 4.15 shows photo catalytic degradation of MB without MFe_2O_4 nanoparticles under visible region (653nm). The intensity is decreased gradually. But there is no shift in absorbance. Solution was kept in sunlight with constant stirring and absorbance was noted after fixed intervals of time. Although, little decrease in intensity was recorded for MB under the exposure of sun light without MFe_2O_4 nanoparticles but no shift in absorbance was recorded, suggesting

the importance of MFe_2O_4 as a photo catalyst. Although, little decrease in intensity was recorded for MB under the exposure of sun light without MFe_2O_4 nanoparticles but no shift in absorbance was recorded, suggesting the importance of MFe_2O_4 as a photo catalyst [2]

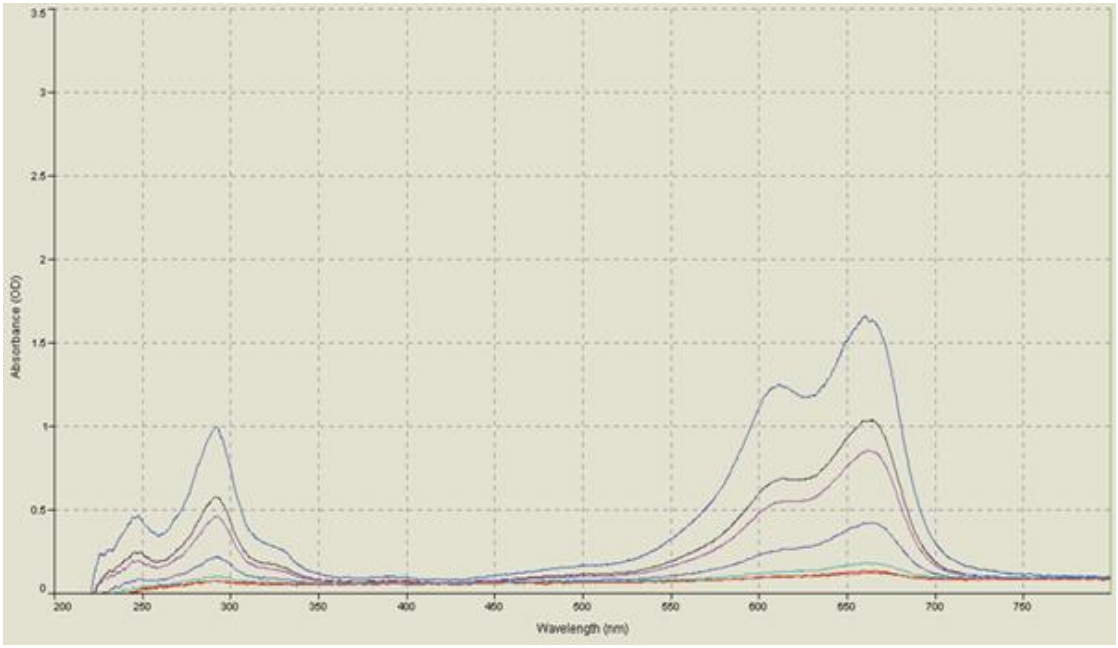

Figure 5.21: Degradation of MB without MFe_2O_4 photo catalyst [2]

Although, little decrease in intensity was recorded for MB under the exposure of sun light without MFe_2O_4 nanoparticles Nano particles but no shift in absorbance was recorded, suggesting the importance of MFe_2O_4 nanoparticles as a photo catalyst.

Figure 4.16 shows the photo catalytic degradation of MFe_2O_4 ferrite nanoparticles. It is seen that the absorbance for the maximum peak at 653nm decreases, indicating the occurrence of the destruction of MB. Green curve is the initial curve with 0hours (degradation time). It shows that concentration of solution is high and absorbance is nearly 3. After degrading slowly absorbance came to around 0.25. It indicates that the color is faded gradually. Extent of MB degradation was estimated from absorbance spectra as intact MB shows strong absorbance at 653nm. Loss of intensity at 653nm and shift in this peak position was considered as degradation of MB. However, exposure of the mixture of MFe_2O_4 ferrite nanoparticles and MB to sunlight resulted in complete degradation of MB within 6hours and the solution becomes colorless. In this case the exposure of MB solution to sunlight alone showed decrease in intensity. The exposure of MB solution under sunlight with MFe_2O_4 ferrite nanoparticles showed a rapid decrease in intensity as well as shift in absorbance. These experiments demonstrated that the presence of both MFe_2O_4 ferrite nanoparticles and sunlight is essential for the degradation of MB. This gives that MFe_2O_4 ferrite nanoparticles degraded MB with 98.6%.

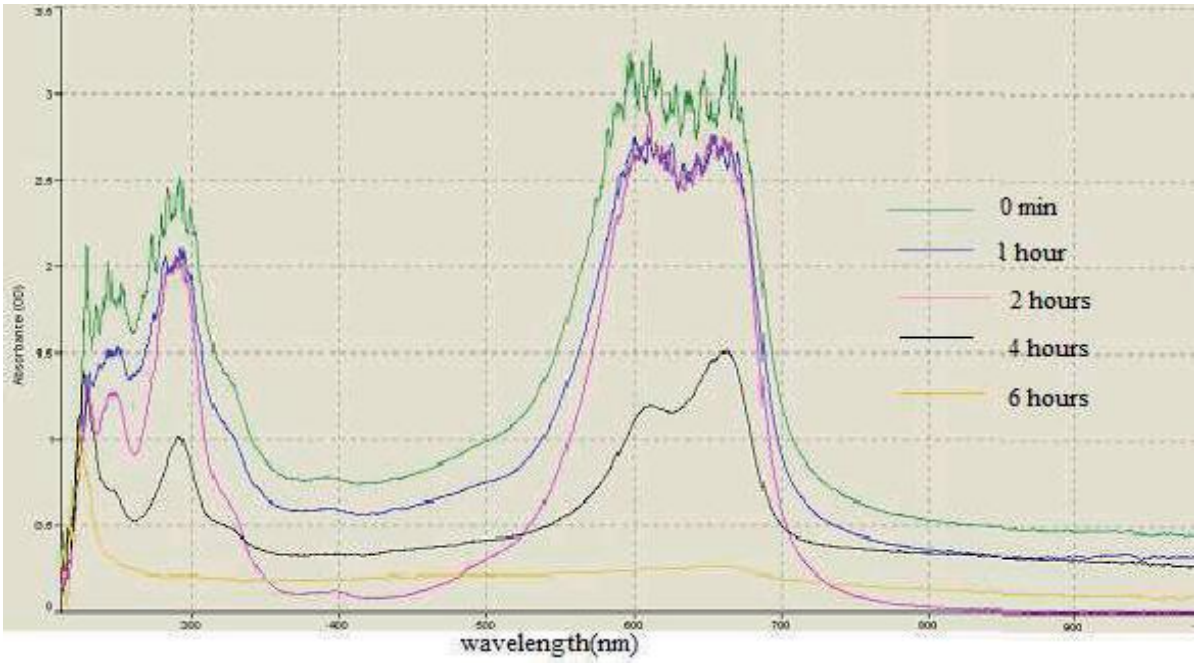

Figure 5.22: Degradation of MB with MFe_2O_4 photo catalyst

CHAPTER 6
CONCLUSION

This Work focuses on the production of green synthesis of ferrite Nano particles (MFe_2O_4). Ferrite Nano Particles (MFe_2O_4) is a well-known photo catalyst. We synthesized Ferrite Nanoparticles via Co-precipitation method by using different plants leaves and their characterization by various techniques that is already mentioned above. This eliminates the need for harmful chemicals, thereby minimizing secondary pollution. The above synthesized samples proved to be efficient materials for degrading contaminated colored waste water using in textile and other dyestuff industry. Hence the synthesized Ferrite nanoparticles prove to be better agents for environmental detoxification of organic compounds, harmful dyes from waste water. Traditional methods for producing ferrite nanoparticles often involve significant resource consumption, long processing times, and the use of harmful chemicals. By contrast, using plant extracts for synthesis offers to explore new, eco-friendly fabrication methods further research is required to evaluate the degradation of real water matrix constituents to better understand practical process applications. This work also focus photo degradation of dye pollutant by using Nano ferrite material also reuse and recycle it by separating it using magnet.

Moreover, future work should aim to enhance nanoparticle efficiency through appropriate doping strategies and by integrating them with other functional materials.

6.1. FUTURE PERSPECTIVES AND CHALLENGES

The advancement of eco-friendly methods for producing ferrite nanoparticles has created numerous possibilities for their application across diverse fields. Despite these promising developments, several challenges and future research areas remain to be addressed:

- Enhancing Synthesis Techniques
- Industrial Scale Production
- Broadening Application Areas
- Assessing Safety and Environmental Impact

REFERENCES

1. Ahmeda, M. H. S. (2017). Introduction to nanotechnology: Definition, terms, occurrence and applications in environment. *Libyan International Medical University Journal*. https://doi.org/10.21502/limuj.003.02.2017
2. Bassa, S., Sanasi, P. D., & Lavanya. (2017). *Synthesis, characterization and photo catalytic applications of ZnO+GO*. Research Scholar, Department of Engineering Chemistry, AU College of Engineering, Andhra University, Visakhapatnam. ISBN: 978-3-330-65142-5
3. Binu, P. J. (2012). *Synthesis of nanomagnetic materials and study of their structural, magnetic and electrical properties*. Department of Physics.
4. Vinodkumar, T., Dinesh, T., Ghosh, K., & Ilavarasan, R. (2025). A comprehensive analysis of minerals in *Moringa oleifera* leaves, seeds, stem bark, and ash using inductively coupled plasma–optical emission spectroscopy (ICP-OES). *Discover Chemistry, 2*, 36.
5. *Azadirachta indica*. (2025, November 9). *Wikipedia, the Free Encyclopedia*. Retrieved November 23, 2025.
6. Win, Z., & Oo, S. S. (2020). Investigation of elemental concentration in neem tree. *Technological University (Pakokku) Journal: Engineering and Research, 2*(1), 452–458. Retrieved November 23, 2025.
7. Kumar, M., Saurabh, V., Tomar, M., Hasan, M., Changan, S., Sasi, M., Maheshwari, C., Prajapati, U., Singh, S., Prajapat, R. K., Dhumal, S., Punia, S., Amarowicz, R., & Mekhemar, M. (2021). Mango (*Mangifera indica* L.) leaves: Nutritional composition, phytochemical profile, and health-promoting bioactivities. *Antioxidants, 10*(2), 299.
8. Dichayal, S., Murade, V., Deshmukh, S., Pansambal, S., Hase, D., & Oza, R. (2024). Green synthesis of cobalt ferrite nanoparticles: A comprehensive review on eco-friendly approaches, characterization techniques, and potential applications. *Journal of Chemical Reviews, 6*(4).
9. Zambri, N. D., Taib, N., Famiza, & Mohamed, Z. (2019). Utilization of neem leaf extract on biosynthesis of iron oxide nanoparticles. *Molecules, 24*(20), 3803. https://doi.org/10.3390/molecules24203803
10. Tejashwini, D. M., Harini, H. V., Nagaswarupa, H. P., Naik, R., Harlapur, S., & Basavaraju, N. (2024). Nanoferrites in photo catalytic wastewater treatment: Advancements, characterization, and environmental implications. *Results in Chemistry, 7*, 101247.

11. Alqassem, B., Banat, F., Palmisano, G., & Abu Haija, M. (2024). Emerging trends of ferrite-based nanomaterials as photocatalysts for environmental remediation: A review and synthetic perspective. *Sustainable Materials and Technologies, 40*, e00961.
12. Shelash, S. I., Khodadadi, A., Shahab, S., Saadoon, S. J., Mengelizadeh, N., Balarak, D., & Al-Zaidy, K. A. M. (2025). Photocatalytic degradation of Acid Blue 113 dye by montmorillonite/copper ferrite nanocomposite: Characterization, optimization, and toxicity assessment. *Chemical Physics Impact, 10*, 100857.
13. Sidhaarth, A. K. R. (2015). *Adsorption of lead zinc and congo red dye from aqueous solution using cobalt ferrite ($CoFe_2O_4$) and manganese ferrite ($MnFe_2O_4$) nanoparticles* (Doctoral dissertation, Anna University). Shodhganga@INFLIBNET.
14. Swapna, K., Murthy, S. N., & Nageswar, Y. V. D. (2011). Magnetically separable and reusable copper ferrite nanoparticles for cross-coupling of aryl halides with diphenyl selinides. *European Journal of Organic Chemistry*, 2011, 1940–1946.
15. Sanasi, P. D., Majji, R. K., Bandaru, S., Bassa, S., Pinninti, S., Vasamsetty, S., & Korupolu, R. B. (2016). Nano copper ferrite catalyzed sonochemical, one-pot three and four component synthesis of poly substituted imidazoles. *Modern Research in Catalysis*, Article ID 62705, 14 pages.
16. Singh, S. (2021). *Envisioning the modifications in spinel nanoferrites for improved characteristics with enhanced catalytic performance for environmental remediation* (Doctoral thesis). Department of Chemistry, Panjab University.
17. Udhaya, P. A. (2021). *Studies on some transition metal substituted spinel ferrite nanoparticles prepared via green synthesis* (Doctoral thesis). Department of Physics, Manonmaniam Sundaranar University.
18. Sunny, A. (2020). *Development of biocompatible spinel ferrite nanoparticles using a facile synthesis for hyperthermia therapy* (Doctoral thesis). Physical Sciences (CSIR-NIIST), Academy of Scientific and Innovative Research (AcSIR).
19. Hariganesh, S. (2021). *Synthesis and characterization of copper based spinel and thiospinel nanocomposites for environmental applications* (Doctoral thesis). Faculty of Science and Humanities, Anna University.
20. Yadav, N., & Ahmaruzzaman, M. (2024). Recent advancements in $CaFe_2O_4$-based composite: Properties, synthesis, and multiple applications. *Energy & Environment, 35*(1), 458–490.

21. Patil, R. P., Delekar, S. D., Mane, D. R., & Hankare, P. P. (2013). Synthesis, structural and magnetic properties of different metal ion substituted nanocrystalline zinc ferrite. *Results in Physics, 3*, 129–133.
22. Kamakshi, T., Sundari, G. S., Erothu, H., & Singh, R. S. (2019). Effect of nickel dopant on structural, morphological and optical characteristics of Fe_3O_4 nanoparticles. *Rasayan Journal of Chemistry, 12*(2), 531–536.
23. Cruz-Espinoza, J. E., Orduña-Díaz, A., Rosales-Perez, M., Zaca-Morán, O., Delgado-Macuil, R., Gayou, V. L., & Rojas-López, M. (2013). FTIR analysis of phenolic extracts from *Moringa oleifera* leaves [Conference paper]. Sociedad Mexicana de Bioquímica, Congreso SMBB, Cancún.
24. Guda, S., & Kala Kumar, B. (2020). Identification of vital phytoconstituents in *Moringa oleifera* (L.) through FTIR spectroscopy. *International Journal of Current Microbiology and Applied Sciences, 9*(12), 3504–3507.
25. George, L. (2021). *Synthesis and characterization of nano mixed ferrites and its photo catalytic application in dye degradation*. Shodhganga.

GREEN SYNTHESIS OF NANO FERRITES FROM DIFFERENT PLANT LEAVES, CHARACTERIZATION AND APPLICATIONS AS PHOTO DEGRADATION ACTIVITY

(ISBN: 978-93-47587-12-2)

About Authors

Rahul Kumar Sahu is currently working as a Senior Loco Pilot in Indian Railways, Government of India. He completed his Master of Science in Environmental Science from Indira Gandhi National Open University (IGNOU) in 2025 with First Division. He also earned a Master of Social Work from Bhoj Open University, Bhopal, in 2023 with First Division. Earlier, he completed his Master of Technology in Thermal Engineering from Rajiv Gandhi Proudyogiki Vishwavidyalaya (RGPV), Bhopal, in 2019 with First Division, and a Post Graduate Diploma in Disaster Management from IGNOU, Bhopal, in 2017 with First Division. Mr. Sahu has professional experience as an Assistant Professor in an engineering college in Bhopal and has also worked as a Mechanical Engineer at a thermal power plant. He has published one book chapter with the national publisher Bhumi Publishing Ltd., India. He has attended several workshops and seminars and has successfully completed multiple professional development courses through the Karmayogi portal, continuously updating his knowledge and skills.

Dr. Bassa Satyannarayana is an Assistant Professor in the Department of Chemistry at Govt. M.G.M. P.G. College, Itarsi, Madhya Pradesh, with over five years of experience in teaching, research, and administration. He serves as the Nodal Officer for SWAYAM courses, College Website Incharge, and Head of the Chemistry Department. He earned his PhD in Chemistry from Andhra University in 2017, specializing in Nano Catalysis and Organic Synthesis. He has cleared multiple national-level exams, including CSIR-UGC-JRF (twice), GATE (five times, ranking 163), and various PSC exams. He has received several accolades, including the Best Academician Award (Elsevier SSRN-2020) and the Vivek Sagar Samman Award. With 7 Indian and 2 Australian patents, 20 research publications, 17 books, and 19 edited books, he has made significant academic contributions. He has also developed e-content under NEP 2020, translated a book into five foreign languages, and actively participates in conferences and workshops.

Bhumi Publishing

ISBN 978-93-475-8712-2

9 789347 587122